ALKOR–Berichte

Bathymetric and microbial investigations at the Grimsey Vent Field (Iceland)

Cruise No. AL595

31.5. – 20.6.2023
Kiel (Germany) – Grimsey Vent Field (Iceland) – Kiel (Germany)
AUV@GVF

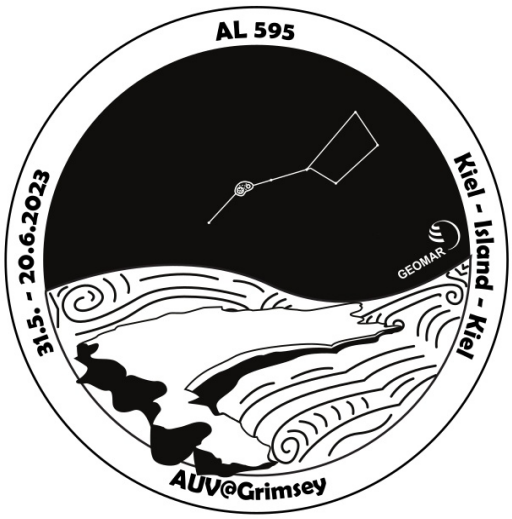

Sebastian Hölz & Mirjam Perner

with contributions from: Nicole Adam-Beyer, Wanda Schmitz, Matthias Türk, Arlette Wenzel-Storjohann, Patrick Leibold, Nikolaj Diller, Anna Jäkle, Torge Kurbjuhn & Danilo Scheppukat

GEOMAR Helmholtz Centre for Ocean Research Kiel

2023

Table of Contents

1 Cruise Summary

1.1 Summary in English

During research cruise AL595 (31.5. - 20.6.2023) onboard research vessel ALKOR, investigations were carried out at the Grimsey Hydrothermal Field offshore Northern Iceland as part of the Helmholtz InnoPool project "High CO_2 – metabolic responses and bioeconomic opportunities". For the first time, the Hover-AUVs *Anton* and *Luise* were successfully operated at water depths of up to 400m, which is close to the maximum operational depth of 500m specified for these Girona 500 AUVs. AUV *Anton* was used to measure high resolution multibeam data with a horizontal resolution of approximately 40cm covering a total area of ca. 1.4km^2. AUV Luise acquired five photo-mosaics with sub-centimeter resolution covering a total area of ca. 5.000m^2. In addition, both AUVs carried CTD probes, which will allow to investigate the local distribution of hydrothermal activity. Both high-resolution bathymetry and photogrammetry data yield new insights into the morphology and overall structure of the vent site and its surrounding, which will be valuable for the interpretation of geophysical data previously acquired in the working area. Sampling with a multicorer (three successful deployments), a 300cm long gravity corer (five successful deployments), a BIGO lander (two successful deployments) and casts with the CTD-rosette (seven deployments) generated fluid, pore-fluid and sediment samples to be analyzed by the working groups Geomicrobiology and Biogeochemistry, Marine Natural Products and Marine Geochemistry at GEOMAR and at Matís (Iceland, Natural Products only). Lab work to be carried out in the home labs will yield insights into the physiological adaptation of microbial communities and individual microbes to very high CO_2 concentrations and will explore microbial utilization of CO_2 for establishing CO_2-based bioeconomic value chains.

1.2 Zusammenfassung

Im Rahmen der Forschungsreise AL595 (31.5. - 20.6.2023) an Bord des Forschungsschiffs ALKOR wurden im Rahmen des Helmholtz-InnoPool-Projekts "High CO_2 – metabolic responses and bioeconomic opportunities" Untersuchungen am Grimsey Hydrothermalfeld vor der Küste Nordislands durchgeführt. Zum ersten Mal wurden hier die Hover-AUVs *Anton* und *Luise* erfolgreich in Wassertiefen von bis zu 400m eingesetzt, was nahe an der für diese Girona 500 AUVs angegebenen maximalen Einsatztiefe von 500m liegt. Mit dem AUV *Anton* wurden hochauflösende Multibeam-Daten mit einer horizontalen Auflösung von ca. 40cm gemessen, die eine Gesamtfläche von ca. 1,4km^2 abdecken. Mit dem AUV *Luise* wurden fünf Fotomosaike mit einer Auflösung im Subzentimeterbereich aufgenommen, die eine Gesamtfläche von ca. 5.000m^2 abdecken. Darüber hinaus wurden mit beiden AUVs CTD Messungen durchgeführt, die es ermöglichen werden, die lokale Verteilung der hydrothermalen Aktivität zu untersuchen. Sowohl hochauflösende Bathymetrie- als auch Photogrammetriedaten liefern neue Einblicke in die Morphologie und Gesamtstruktur des Hydrothermalfeldes und seiner Umgebung, die für die Interpretation der zuvor im Arbeitsbereich erfaßten geophysikalischen Daten hilfreich sein werden. Die Probenahme mit einem Multicorer (drei erfolgreiche Einsätze), einem 300 cm langen Schwerelot (fünf erfolgreiche Einsätze), einem BIGO-Lander (zwei erfolgreiche Einsätze) und dem Kranzwasserschöpfer (sieben Einsätze) lieferten Flüssigkeits-, Porenflüssigkeits- und Sedimentproben, die nach unserer Rückkehr von den Arbeitsgruppen Geomikrobiologie und Biogeochemie, Marine Naturstoffchemie und Marine Geochemie am GEOMAR und bei Matís (Island, nur Natural Products) analysiert werden. Die in den Heimlaboren durchzuführenden Laborarbeiten werden Einblicke in die physiologische Anpassung mikrobieller Gemeinschaften und einzelner Mikroben an sehr hohe CO_2-Konzentrationen liefern und die mikrobielle Nutzung von CO_2 für den Aufbau CO_2-basierter bioökonomischer Wertschöpfungsketten untersuchen.

2 Participants

2.1 Principal Investigator

Name	Institution
Hölz, Sebastian, Dr.	GEOMAR

2.2 Scientific Party

Name	Discipline	Institution
Hölz, Sebastian, Dr.	geophysics, chief scientist	GEOMAR
Perner, Mirjam, Prof. Dr.	microbiology, co-PI	GEOMAR
Adam-Beyer, Nicole, Dr.	microbiology	GEOMAR
Schmitz, Wanda	student aid geochemistry / gravity coring / microbiology	UHH
Türk, Matthias	technician, BIGO	GEOMAR
Wenzel-Storjohann, Arlette	marine natural products	GEOMAR
Klonowski, Alexandra	marine natural products	matís
Jäkle, Anna	electrical engineer, AUV	GEOMAR
Leibold, Patrick	software engineer, AUV	GEOMAR
Diller, Nikolaj	software engineer, AUV	GEOMAR
Kurbjuhn, Torge	technician, AUV	GEOMAR
Scheppukat, Danilo	electrical engineer, AUV	GEOMAR

Fig. 2.1 Group pictures taken at the start of the cruise on May 31st just after entering the Kiel Canal (top) and shortly after our return to Kiel during demobilization on June 19th (bottom).

2.3 Participating Institutions

GEOMAR	GEOMAR Helmholtz Centre for Ocean Research (Kiel, Germany)
UHH	University of Hamburg (Hamburg, Germany)
matís	Matís ohf. - Icelandic Food and Biotech R&D (Reykjavik, Iceland)
RPS	RPS Energy Canada Ltd. (Calgary, Canada)

3 Research Program

(Sebastian Hölz & Mirjam Perner)

3.1 Description of the Work Area

3.1.1 Introduction

Hydrothermal circulation is driven by heat and occurs mainly at marine plate boundaries such as mid ocean ridges (MOR), volcanic arcs and at back arc basins where heat is supplied by increased magmatic activity. In places where hydrothermal circulation of seawater leaches metal ions out of the host rock, mineral enriched fluids can rise towards the seafloor where they cool and precipitating metals may form seafloor massive sulfide (SMS) sites. Depending on the structure of the seafloor and the overall buildup of hydrothermal circulation, the cooling of hydrothermal fluids may occur within the seafloor causing the deposits may form at depth or within the water column, in which case venting of high-temperature fluids may build up chimney structures such as black smokers. Along oceanic plate boundaries approximately 330 vent sites have been observed at the seafloor. Of these sites, a majority of 237 contain massive sulfide mineralization (Beaulieau et al., 2015; Monecke et al., 2016). The estimate of the global potential yields a total accumulated volume of 600 million tons of SMS containing 30 million tons of copper and zinc, which are present in the immediate vicinity of the oceanic plate boundaries (Hannington et al., 2010 & 2011). Due to the fact that SMS are compact structures close to the seafloor with potentially high ore grades, the possibility of mining such SMS deposits has gained much attention on a national and international level (Boschen et al., 2013).

Along the Arctic Mid-Oceanic Ridge (AMOR), which runs from the northern coast of Iceland along the Kolbeinsey, Mohns and Knipovich Ridge (Fig. 3.1) and further North, several hydrothermal vent fields have been confirmed (Beaulieu, 2015; Pedersen et al., 2010a). The Grimsey Vent Field (GVF) is the southernmost known active vent field along the AMOR showing high temperature venting above 250°C (Hannington et al., 2001). With spreading rates of less than 20mm/a, the site is hosted on an ultra-slow spreading segment of the ridge (Snow & Edmonds, 2007). German et al. (2016) state that there is an “excess” of high temperature venting along slow and ultra-slow spreading ridges and conclude that ultra-slow ridges may represent the strongest mineral resource potential for the global ridge crest.

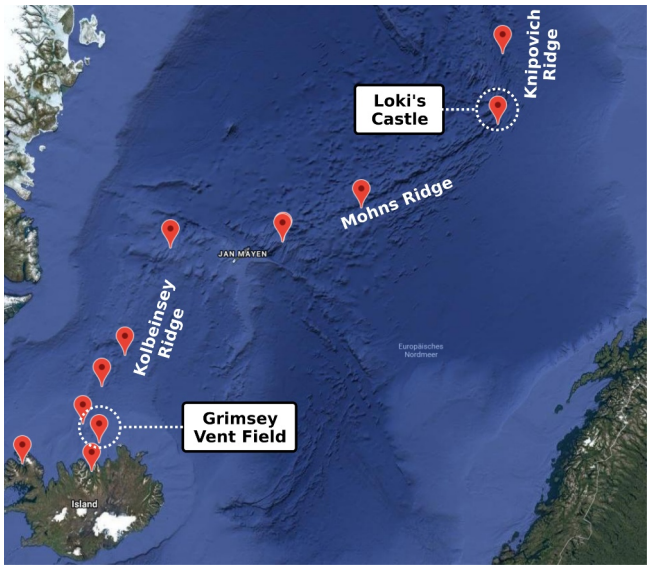

Fig. 3.1 Arctic Mid-Oceanic Ridge (AMOR) with the proposed working area Grimsey Vent Field (GVF) and additional vent fields (Beaulieu, 2015).

Substantial knowledge can be gained by the study of hydrothermal systems and/or SMS sites on ultra-slow spreading ridges when observations are coupled with suitable experiments espe-

cially with regards to the genesis and development of such sites. For example, information on a physical, bio-geochemical, structural and geotechnical parameter are essential data for future target-oriented drilling. Furthermore, the comparison to previous experiments conducted at sites located at slow-spreading ridges (e.g. Shinkai & Double Mound, MIR Zone, cruise JC138, 2016) or in an island-arc setting (e.g. Palinuro, cruises POS483 & POS509) could also add to the understanding of SMS sites in these various geological settings.

From the perspective of understanding fundamental features of biology – including evolutionary processes in deep time – hydrothermally influenced habitats and mineral deposits themselves select for local microbial community compositions that reflect life in extreme environments including life before Earth's oxygenation. Microbial processes also contribute to the formation and conversion of the mineralogical composition as well as fluid chemical compounds. Thus, a strong tie between microbe-mineral interactions and biogeochemical cycling is obvious. Over the years, several microbiology studies on phylogenetic and functional diversity and turnover rates have been performed. They dealt with elucidating bio-geo-coupling processes between the abiotic and biotic world along MORs in the Atlantic, the Pacific and the Indian Ocean as well as volcanic island arc systems (e.g., Huber et al., 2010; Perner et al., 2013a; Perner et al., 2013b; Gonnella et al., 2016; Olins et al., 2017; Han et al., 2018; Boehnke-Brandt et al., 2019). Albeit, generally relatively little has been done in hydrothermally influenced habitats with respect to searching for microbially produced bioactive secondary metabolites affecting microbial activity and describing their role in the given habitat (Kicklighter et al., 2004; Eythorsdottir et al., 2016; Shi et al., 2017; Gutierrez-Almada et al., 2020).

To our knowledge, no peer-reviewed article on microbial community compositions and functionality for the Grimsey vent field has been published to date. The only available information can be found in the cruise report of cruise POS291 (Devey, 2002) and a PhD thesis by Hobel (2004), which claims a dominance of thermotolerant, thermophilic and hyperthermophilic species where the majority of 16S rRNA genes appears to be associated with Epsilonproteobacteria and Thermococcales at Grimsey. Nevertheless, these microbes are commonly found in chemically distinct venting environments and no further details on diversity or functionality are given. In contrast, for the Loki's Castle vent field at the NE end of the AMOR, several microbial community assessments and thermodynamic models have been conducted (Dahle et al., 2013; Dahle et al., 2015; Stokke et al., 2015; Steen et al., 2016). There, the discovery of a novel uncultured Archaea in a gravity core of muddy venting sediments (Pedersen et al., 2010b) later led to revolutionizing our ideas on eukaryogenesis. Members of this uncultured archaeal group were named Lokiarchaeota and are now proposed to bridge the evolutionary gap between simpler microbes and eukaryotes (Spang et al., 2015; Imachi et al., 2020). Consequently, the shallow GVF with its extensive subsurface boiling system, its emitting gas-charged bubbles and fluid-sediment interactions with methane and higher hydrocarbon enrichments (Botz et al., 1999) mark an interesting site for studying microbial life, its adaptations and development.

3.1.2 Geological Target – Grimsey Vent Field

On Iceland, occurrences of high-temperature hydrothermal systems are clearly linked to the neovolcanic zone (Fig. 3.2), which crosses the island from the SW to the NNE. The neovolcanic zone is an expression of the Mid-Atlantic Ridge system crossing the Iceland hot spot (Hannington et al., 2001). As part of the system, the neovolcanic zone extends into the submarine domain to the SW along the Reykjanes Ridge and to the NNE along the Kolbeinsey Ridge. The Grimsey Hydrothermal Field (GVF) is located in the Grimsey Graben, a pull-apart basin within the Tjörnes Fracture Zone (see Fig. 3.2). The depression is about 10 km wide, 30–40 km long and filled with glacial sediments from ice-fed rivers draining the north coast of Iceland (Lackschewitz et al., 2006). Seismic and geochemical investigations indicate high permeability in the deep crust, which facilitates fluid and gas migration from the crust–mantle boundary to the seafloor (Riedel et al., 2001).

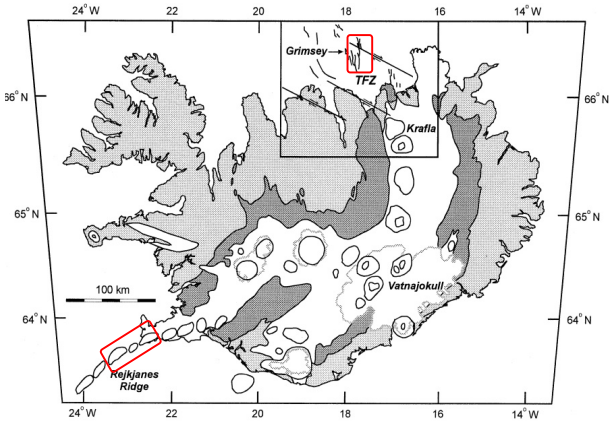

Fig. 3.2 Map of Iceland (from Hannington et al., 2001) showing the neovolcanic zone (white) with offshore extensions to the SW along the Reykjanes Ridge, to the NNE in the Tjörnes Fracture Zone (TFZ) and the Kolbeinsey Ridge. The red box to the North marks the approximate extent shown in Fig. 3.3.

Initial research at the GVF was carried out during *R/V POSEIDON* cruises POS229, POS253 and POS291 (1997, 1999, 2002, respectively). During these cruises Hannington et al. (2001) identified 24 mounds and chimneys in JAGO dives, of which 14 are characterized as high-temperature vents (boiling). They also show acoustic scattering within the water column in echosounder profiles (their figure 5), which they used to map out the extent of the hydrothermal field. Fluid analyses on core samples are reported with end-member chlorinity of 274mM, which is about half of seawater chlorinity (Lackschewitz et al., 2006). Even though sulfur smell was apparent on fresh chimney samples, the lack of smoke in the venting fluids and the only patchy distribution of bacteria mats on the surfaces of mounts suggests that neither sulfur nor metals are abundant at the surface. However, it remains unclear if accumulations of massive sulfides may exist at greater depth (Hannington et al., 2001).

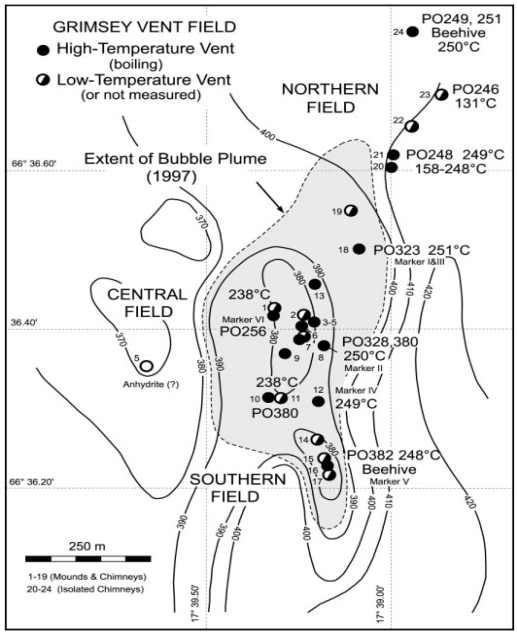

Fig. 3.3 Contour map of the GVF with locations of temperature measurements and the area (shaded) of active, high-temperature venting (Hannington et al., 2001).

Some additional geophysical data is presented by Magnúsdóttir et al. (2015), who show an E-W striking section of chirp seismic data, in which the GVF is associated with two separate, cone-

shaped acoustic anomalies along a stretch of about 500m. This is a first indication that the vent field is actually larger than depicted in Fig. 3.3 and may actually consist of several separate centers of strong hydrothermal activity. They also present some stratigraphy from the approximately 38m long drill core MD-75, which was taken at a location about 6km to the SSW of the GVF. Additional information about this core can be found in Gudmundsdóttir et al. (2011).

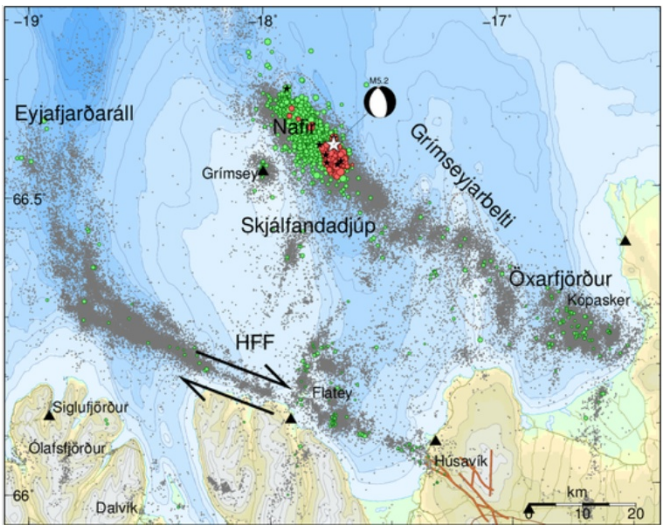

Fig. 3.4 Seismic activity offshore northern Iceland (gray: since 1994, green: January 2018, red: since 19.2.2018) measured with a seismic network (black triangles). Magnitude larger 4 are shown as black stars, the white star indicates the location of a M5.2 earthquake (IMO, 2018b).

News in the year 2018 reported that the area around the GVF was shaken by swarms of earthquakes. The highest activity with about 2000 events was reported mid February[1] (IMO, 2018a). The Icelandic Met Office (IMO, 2018b) reports the highest activity on February 19th with the largest earthquake (M5.2) located 14km ENE of Grímsey together with five smaller earthquakes (M4-4.9). Shorty before our cruise, several smaller earthquakes with magnitudes between 2.8 – 4.2 were reported in local newspapers (visir, 2023; Morgunbladid, 2023, Rúv, 2023). Generally, such pattern of activity occur every few years with similar activity reported in May and September 1969, during the Christmas period in 1980, in September 1988 and April 2013.

3.1.3 Previous work at GVF

The Grimsey Vent Field was the main research target during cruises POS524 (Hölz & Martins, 2018) and POS535 (Hölz et al., 2019). Our work focused on electromagnetic (EM) investigations, measurements with a 220cm long heat-probe and sampling with a 280cm long gravity corer (GC).

During both cruises, several EM experiments with complementary depths of investigation (DOI) and varying lateral resolution were carried out. The processing of data from the TEM and Coil2Dipole experiments have been partially finished and first inversion results give an interesting and somewhat unexpected insight into the internal structure of the hydrothermal field. A pseudo-2D-section of TEM data (not shown) gives some evidence of elevated conductivities (3 – 5 S/m) in the vicinity of the active field. However, the most striking feature is an extended good conductor to the W of the active field, which exhibits significantly higher conductivities of around 10S/m and above, starting at a depth of about 15 – 20m beneath the seafloor.

Generally, such high conductivities can be explained by a combination of high temperature saline fluids, which could migrate from basement depths towards the seafloor along existing west dipping faults (Riedel et al., 2001), and / or mineralizations, which can precipitate as fluid temperatures drop, e.g. due to the contact with cold seawater. At the moment it is unclear how

1 http://icelandreview.com/news/2018/02/19/magnitude-52-earthquake-near-grimsey

the good conductor to the west of the active vent field is actually connected to the vent field. Especially, it is unclear why no surface expressions of hydrothermal venting like chimneys are evident in this area and no temperature anomalies or active venting could be found in this area.

3.2 Aims of the Cruise

In order to better understand the geological framework of the working area and to facilitate the interpretation of the previously acquired geophysical and geological data, we proposed to perform AUV tests in a working area. While our first results of electromagnetic methods in combination with heat flow measurements, gravity coring and fluid sampling from previous cruises hinted towards a potential massive mineralization within the seafloor to the West of the active GVF, the interpretation was limited by the rather low-resolution of the currently available bathymetry (10m lateral resolution) and the lack of visual coverage. Consequently, the testing of AUVs at greater water depths was also aiming to yield scientifically meaningful data valuable for the interpretation of our previous experiments by allowing for an improved structural interpretation (high-resolution bathymetry, photogrammetry). Additionally, a high-resolution bathymetry would also be essential for planning of target-oriented drilling in the scope of a potential future MeBo drilling proposal. Generally, complex measurement platforms like GEOMAR's recently acquired Hover-AUVs *Anton* & *Luise* require substantial testing in suitable working areas in order to be successfully integrated into an institute's infrastructure. During cruise AL533 (Hissmann et al., 2020), the AUVs' navigation units (e.g. INS, DVL) and underwater communication platform (BELUGA) as well as acoustic transponders needed for a long baseline (LBL) network, were already successfully tested in water depths up to 200m.

Therefore, AUV testing and measurements focused on the following goals:

- operation of AUVs close to the maximum operational depths of 500m,
- operation of AUVs in stationary LBL network,
- acquisition of high-resolution bathymetry (~50cm lateral resolution or better on an area of approximately 2km^2),
- acquisition of additional data with external sensors (e.g. photogrammetry, magnetics) and other available sensors. The acquisition of magnetic data was considered as a low priority task and – in the end – was not carried out because AUV *Luise* was not operational during the last days of the cruise.

We also aimed to broaden the scope of investigations to include methods, which have previously not been performed in the working area or have never been published. With its extensive subsurface boiling system emitting gas-charged bubbles and fluid-sediment interactions with methane and higher hydrocarbon enrichments (Botz et al., 1999), the vent field marks an ideal site for studying microbial life, its adaptations and development. To our knowledge, the last and only microbial study at the GVF was carried out more than 20 years ago during cruises POS253 (Scholten, 2000) and POS291 (Devey, 2002) and results have only been published as part of a PhD thesis (Hobel, 2004). Therefore, the substantial methodological and scientific advances of life sciences in the past decades have not been applied to microbial communities at the GVF. The proposed microbial studies aim to perform a baseline study on microbial activity in the shallow

sediments (<3m) to be sampled with MUC, GC and BIGO lander. More specifically, microbes from the three domains of life – eukaryotes, bacteria and archaea – will be sampled. Coordinated sampling of these communities is still rare, and we are yet to understand the full biogeochemical processing and microbial exchanges, as well as gaining new insights into evolution in deep time. For this, integrated studies are essential. To this end, we will perform DNA and – if sufficient biomass is available – RNA extraction and illumina sequencing of 16S RNA gene (bacteria and archaea) and 18S rRNA (eukaryotes) amplicon sequencing for analyses of the microbial community. Omic tools can be applied to these samples within other research projects. Enrichment cultures will be set up targeting chemosynthetic microorganisms and heterotrophs producing natural products. This study will provide a good frame work for later in depth and extensive analyses of bio-geo-coupling processes based on in-situ experiments. Results are expected to contribute to the Helmholtz InnoPool project "High CO_2 – metabolic responses and bioeconomic opportunities", in which FZ Jülich, GFZ Potsdam and GEOMAR are collaborating to study physiological adaptation of microbial communities and individual microbes to very high CO_2 concentrations and explore microbial utilization of CO_2 for establishing CO_2-based bioeconomic value chains.

As part of the future drilling proposal, this work would then be extended to greater depths up to approximately 50m to also yield novel insight into the vertical distribution patterns of microbial life and its interaction with the hydrothermal system.

3.3 Agenda of the Cruise

Sailing from Kiel to the working area North of Iceland and back (Fig. 3.5) meant two transits across the North Sea of about five to six days each. Since we had received all necessary permits just in time shortly before starting in Kiel on May 31st 2023, only minor adjustments of our original planned field work were necessary. After arriving in Iceland, we picked up our Icelandic colleague Alexandra Klonowski on June 6th. Contrary to our previous cruise POS535 (2019), where we had chosen Akureyri as port of embarkation, we this time used the port of Dalvik, which is about 2h closer to the working area (one-way). The same port was also used for the disembarkation and stashing of fuel on June 13th. It proved to be well suited for these purposes and should be considered as good alternative for future field work at the Grimsey Vent Field.

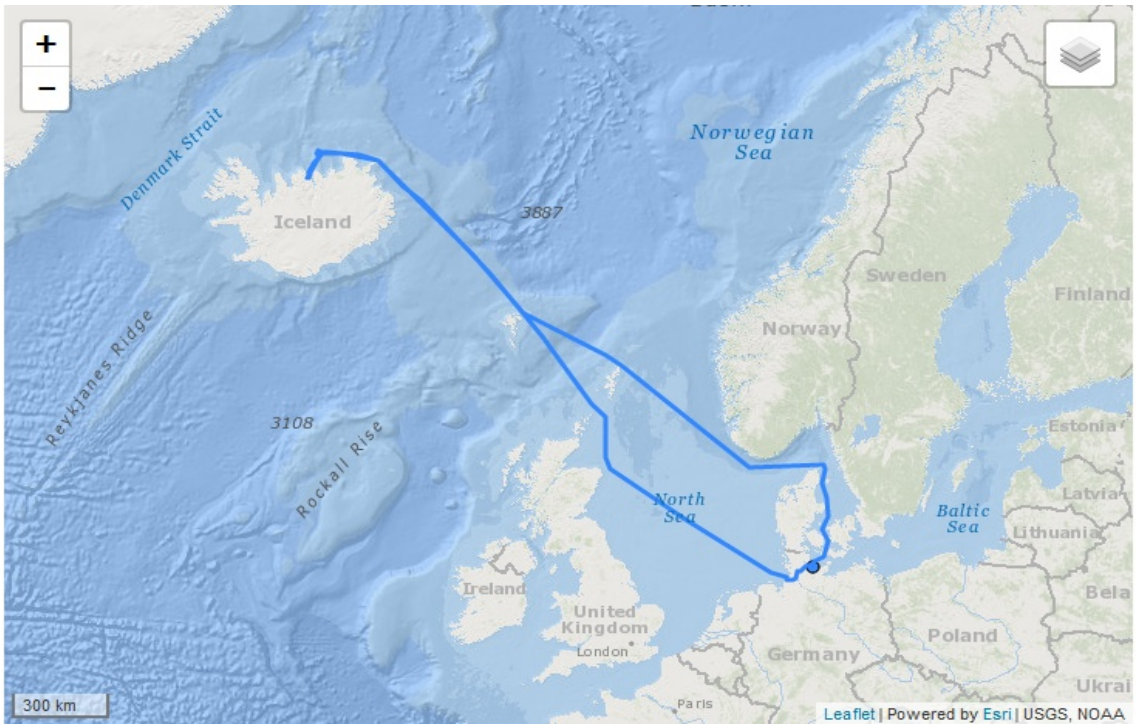

Fig. 3.5 Ship track of RV ALKOR during cruise AL595 from Kiel (Germany) to northern coast of Iceland and back (maps.geomar.de/mapgen_ds/maps/legMap?render=true&leg=AL595).

All research activities were carried out in accordance with the declarations on responsible marine research (Appendices 1 to 3 of the Cruise Proposal Preparation Instructions). Mitigation measures as outlined in Appendix 3 of the proposal instructions were not needed, as no seismic work was carried out during the cruise.

4 Narrative of the Cruise

All times are ship time (UTC + 2h).

On 31.05.2023 we left Kiel around 8:30h in the morning and – after picking up a pilot – entered the North Sea and Baltic canal. After finishing the familiarization with the ship and the mandatory safety drill, the rest of the day was spent with the preparation of laboratories and equipment on deck. In the evening hours we left the canal and entered the North Sea. The expected travel time to the working area offshore Northern Iceland is about six days.

1. - 2.6.2023: Due to strong winds and heavy waves, preparations were essentially stopped for the day. Everyone is hoping for better weather conditions for tomorrow.

3.6.2023: After a couple of rough days, the last night was finally quiet again and everyone finally got some rest. Today, we set up the laboratories and started to coordinate the sampling procedures for the work on the core carried out for analyses for microbiology, geochemistry and natural products. In the evening hours we are somewhere between the Britain and the Faeroe Islands, hoping that the sea will remain calm.

4.6.2023: Around midnight we have passed the Faeroe Islands. Together with the midnight sun they make for a spectacular sight. After some wind and waves around noon the sea calms down. In the afternoon, most preparations for the upcoming experiments are finished.

5.6.2023: In the morning hours we arrive on the easterly coast of Iceland and, after sailing around the NE tip, finally reach the working area in the early afternoon around 15:00h. With a first CTD cast we start the scientific experiments of the cruise. Afterwards, the AUV crew performs a first dipping test with the AUVs to test the buoyancy and trim of the vehicles. Since everything works out just fine, a first dive with the AUV *Anton*, which carries the multi-beam, is carried out to the seafloor. Communication, DVL, multi-beam and the other systems seem to work just fine. It looks like we are good to go for tomorrow!

6.6.2023: Our first day in the working area is dedicated to sampling: first we take our first samples with the Multicorer (MUC, station MUC01) with full recovery on all twelve liners. We have chosen an area about 4km to the West of the active vent site in order to collect some background material for the natural products group. Afterwards we prepare work in the main working area above the vent field by taking a first CTD above the assumed first deployment site for the BIGO lander. The afternoon is then dedicated to the BIGO lander. Our plan is to lower the lander to the seafloor and then traverse the vent site from SE to NW in order to find a suitable spot for the deployment. With the lander close to the seafloor we see that live feed from the seafloor is difficult. Even though we can sometimes see the seafloor, the heave of the ship prevents us from identifying a good patch of microbes on the seafloor. In the end we deploy the lander just to the West of the active site to leave it there for the next three days. Afterwards, we transfer to Dalvik, which is about 4h away to pick up Alexandra Klonowski (Matís), who will join us for the cruise.

7.6.2023: After deployment of acoustic transponders, which are used to set up an acoustic network for LBL navigation on the seafloor, we deploy the Hover-AUV *Anton* for the first time. During this cruise, *Anton* will be responsible to measure bathymetry with the aim of providing us with high resolution maps of the seafloor with a resolution of a few decimeters. A first test

shows that the AUV has to be operated at an altitude of at maximum 25m above the seafloor in order to ensure that the DVL system locks onto the seafloor. This is needed to ensure a stable navigation of the system. Afterwards, the AUV starts into its first mission delivering us a spectacular map of a part of the vent field with a horizontal resolution of about 40cm. While *Anton* was on its' way, we also found the time to take a first gravity core (GC01) at the same location where we had previously taken the first MUC. Again, the aim is to take some background material in order to coordinate the different working groups and see how the lab work can be organized. In the end, lab work is finished well after midnight.

8.6.2023: The day starts with a CTD and a MUC at a site just NW of the vent field for the natural products group. Afterwards, we deploy the AUV *Luise* for the first time, which will be taking photos of the seafloor that in post-processing can be stitched together to form mosaics of the seafloor. The first part of the mission is a field test to determine how high above the seafloor *Luise* can fly while still delivering well illuminated picture. In the evening we will find out that about 2m above the seafloor (camera elevation) is the maximum elevation where acceptable pictures are still available. After lunch we work on taking a first GC in the center of the vent field. We use transparent liners, which enable us to check the core after recovery in order to decide if we want to keep it or discard it. In our first try (GC02) we get about 1m of material, which looks similar to the background material we have found in GC01, even though measurements in the core catcher already indicate elevated temperatures of 31.4°C. We decide to keep this core on the shelf for the moment and take a second core about 15m to the North of the first core. This core (GC03) comes up from the seafloor with boiling fluids and white material (anhydrite ?!) falling out of the core barrel. Upon inspection we see that this core also contains about 1m of material with several layers of different material. Since we only have the capacity to handle one core and also are limited by the laboratory equipment, we decide to continue work on core GC03. Work continues until the evening hours.

9.6.2023: After the deployment of two transponders for the LBL network, one transponder is currently not operational, AUV *Anton* started its' mission to complete the bathymetric measurements above the active vent field. After recovery in the afternoon, a patch of 450m x 650m, which equals about 0.3km^2, is downloaded and currently being processed. Later in the morning we also deployed AUV *Luise* on a photogrammetry mission with focus on three sites with "holes" in the seafloor. Because we previously found out that the AUV has to be operated fairly close to the seafloor for theses photo-missions (~2m above the seafloor) we are not planing to operate it to work on the active sites. The first depression inspected by *Luise* is then also taken as site for CTD, MUC and GC (GC04). With the MUC we did not recover any material, because the winch cable got entangled in its structure causing slight damage on one of the probing mechanisms. However, with the GC we recovered about 1.6m of core material which shows elevated temperatures at the bottom (15.4°C) and some hydrothermal influence in the lower section.

10.6.2023: First thing in the morning we recover BIGO without any problems. Upon inspection we see that both chambers did close and recovered sediments. The additional experiments also seemingly worked except for the automated sampling with syringes. The rest of the day the people from the microbiology group are busy with taking samples and preparing the BIGO lander for the next deployment. Also in the morning, the AUV team first deployed the transponders

and AUV *Anton* for a mission across the westerly normal fault. The following deployment of AUV *Luise* after lunch at first seemed to go according to plan, but due to strong winds and high waves, the ship lost connection to *Luise* and the required positioning of the AUV was not possible anymore. The emergency system fired, sending *Luise* back to the surface, but due to missing navigation support fixes, the AUV drifted away, thus, leaving the range of the ship. While the AUVs do have an Iridium system to send GPS positions via satellite, the GEOMAR mail-server, to which these messages are directed, is down for maintenance over the weekend. Calls to the hot-line of the Iridium provider solve this problem after a few hours, but valuable time was lost and we are left with an old position. While sorting out these problems, we recover *Anton* and the two transponders (~30min) and later deploy BIGO to the central vent field, where we find a nice patch of bacterial material and place BIGO right on top of it. At about 21h it becomes more and more clear that we will most likely not receive any positions of Luise. Instead, we will have to continue the night with the rescue mission, solely relying on visual inspection of the sea surface and the last positional fix with 4km uncertainty, which we received around 17h.

11.6.2023: In the morning hours we are still running search patterns in our quest to find *Luise*. The AUV team with some support from science and crew have stayed up all night scanning the sea. Unluckily, the midnight sun prevents the flash light from being of any use. A plan of using the drone is worked on, but our hopes of finding *Luise* are fading away when suddenly, around 10h the AUV is finally spotted. Even though it is only about 300m away, it is hard to see, but now that we have it in sight, the rescue is a bare formality. We are all more than happy that this rescue mission has come to a happy ending. Around noon we take a last background sample at the site of CTD01 for our Icelandic colleague, who needs some more bottom water for here analyses. Afterwards, we start the transfer to Dalvik, where she will leave the ship tomorrow. Since waves are supposed to pick up considerably during the day well until tomorrow, we have decided to use Monday for her disembarkment and also to bunker some fuel. This will also give us some time to get some well deserved rest.

12.6.2023: Due to bad weather conditions in the working area, we will stay in Dalvik for the day. Alexandra Klonowski is leaving the ship around noon and the bunkering operation is set to take place in the late afternoon. This day will give us some much needed rest after the long rescue operation. Tomorrow in the early morning hours we will steam back to the working area to commence our work for the last two working days of the cruise.

13.6.2023: After returning to the working area, we deployed *Luise* first thing in the morning. Based on our previous experience, we decided to not run *Anton* in parallel. Targets were the site BIGO_01 and a small structure just to the north of it. With Luise deployed, we sampled with CTD, MUC and GC corer at a location in the middle of several vents. The recovered cores were hot (81°C in the GC core catcher) and were sampled for the rest of the day in the labs. Around noon, *Luise* was recovered and after lunch *Anton* was deployed for its 5th dive to cover the area to the SW, thus, completing our high-resolution bathymetric map of the main working area.

14.6.2023: In the morning, we deployed *Anton* on its last mission in an area ca. 3km to the N of the main working area. We had previously taken samples at this location during the POSEIDON cruise POS524 and also carried out an EM experiment there. After the recovery of *Anton* around noon, BIGO was released and successfully recovered with both chambers full of material showing excessive degassing, strong H_2S smell and plenty of material to sample. This time, all

experiments did work and the rest of the day was spend sampling. As final operation of this cruise, we took the last GC (GC06) at a location on the westerly normal fault, which looked promising on the new high-resolution bathymetric map. With 60cm of recovered material, the scientific program in the working area was finished and ALKOR immediately started to sail back home.

15.6.2023 – 19.6.2023: On the transit back home, we again passed the west-coast of Iceland, the Faeroe and Shetland Islands and then took the route around Skagen and eastern Denmark to arrive in Kiel in the afternoon of June 19th.

5 Preliminary Results

The sampling carried out with CTD, MUC, GC and BIGO during this cruise, generated material for geomicrobiology, biotechnology and geochemistry. Most analyses of collected samples will be carried out after the cruise at the involved institutes. While the individual lab methods may vary for these research fields, the initial sampling from the seafloor and chosen locations were often identical. Fig. 5.1 gives an overview of the sampling locations. Please note that the some samplings were taken at the same location: GC01 | MUC01 | CTD01 & CTD06 (all not shown on map), GC04 | MUC03 (no recovery in MUC), and finally GC05 | MUC04 | CTD07. The initial sampling from or at the seafloor is described in the instrumentation chapter 5.1. Details about individual sampling procedures of the various methods and – where available – first results are summarized in following chapters 5.2 – 5.4. A complete table of all stations and tables for individual methods can be found in chapters 6.1 (p. 37ff) and 6.2 (p. 39ff).

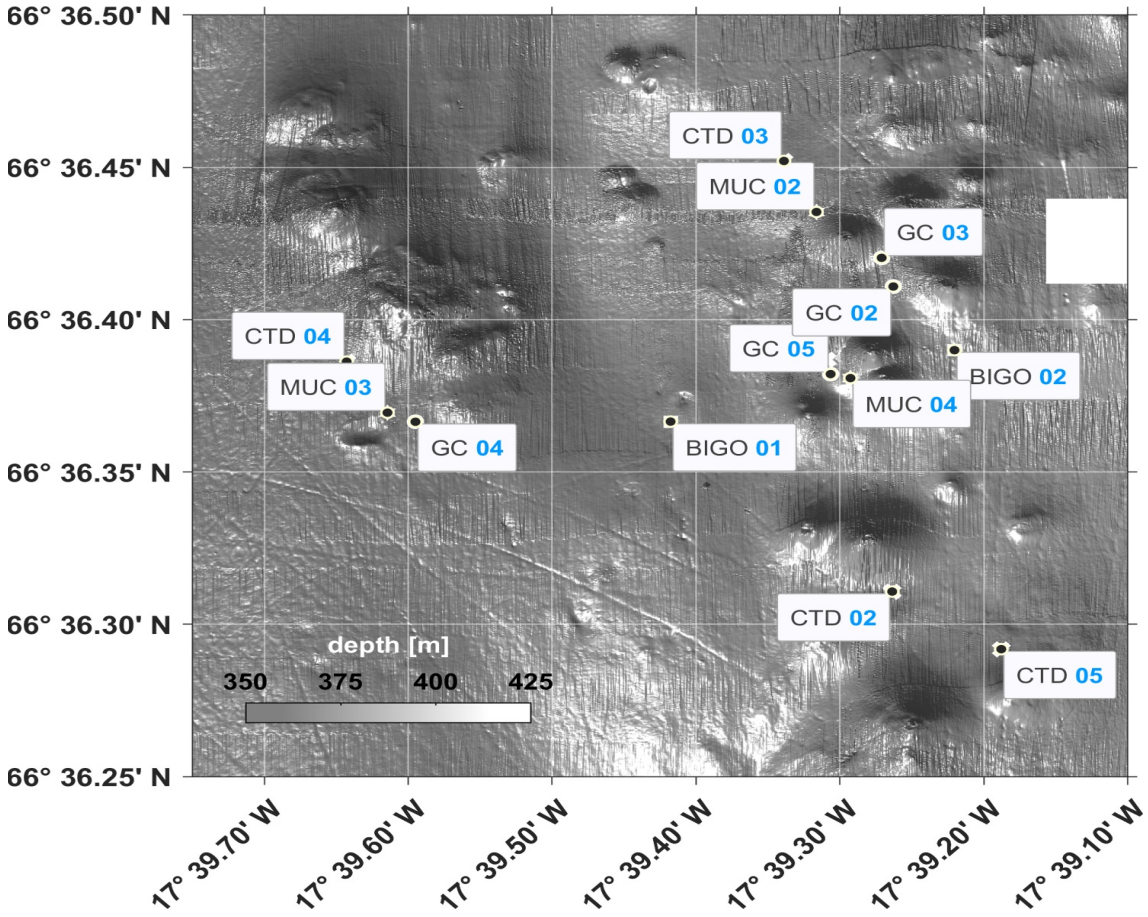

Fig. 5.1 Sampling locations for water sampler with attached CTD sensor (CTD-rosette), gravity corer (GC), multi-corer (MUC), and BIGO lander during cruise AL595. GC01 and GC06 were taken outside the map shown here to the west of the active vent sites. Please note that some samplings were taken at the same location: GC01 | MUC01 | CTD01 & CTD06 (all not shown on map), GC04 | MUC03 (no recovery), and GC05 | MUC04 | CTD07.

5.1 Instrumentation for Marine Sampling and General Sampling Procedures

(Nicole Adam-Beyer, Arlette Wenzel-Storjohann, Mirjam Perner, Wanda Schmitz, Matthias Türk)

5.1.1 CTD

The objective of water sampling in the water column was to provide background water samples for geochemical and biotechnological analyses above or in the vicinity of sites where sediment samples were taken, and to provide a velocity profile for the AUV operations. The ship provides the multi-water sampler (Kranzwasserschöpfer) MWS 622 by the company Hydro-Bios (Kiel, Germany) with a maximum operational depth of 3000m. It allows to remotely take water samples at depth from the lab into twelve Niskin bottles, each with a volume of 10l. The attached CTD sensor (type unknown) allows for online measurements of electrical conductivity (C), temperature (T), pressure (P), Chlorophyll and Oxygen. The parameters C,T,D are used to derive additional parameters like salinity or sound velocity. Samples were always taken on the way up with all bottles being closed before recovery.

Fig. 5.2 Multi-water sampler MWS 622 before first deployment (June 5th).

The CTD was used at a total of seven stations for the recovery of water samples (CTD in Fig. 5.1, CTD01 and CTD06 are at the location of GC01 (not shown on the map), CTD04 is at the location of GC04 and CTD07 is at the location of GC05). For sampling, the instrument was first lowered to 10m above the seafloor at a speed of 0.5m/s and then slowed down to 0.2m/s until ground contact. It was then lifted up 1m before the first water samples were taken. On some sites, all bottles were closed while on other sites we collected profiles of water samples with a spacing of approximately 40m. A table with all CTD casts can be found in chapter 6.2.1 (p. 39).

Additionally, we used an autonomous CTD (CTD48M by Sea & Sun Technology) with a maximum operational depth of 1000m. This probe was only used once, when it was attached to the BIGO lander during the deployment at station BIGO_02.

5.1.2 GC

The objective of sampling with the gravity corer (GC) was to obtain sediment and pore water samples down to a depth of at maximum 300cm to be analyzed by the geomicrobiology, biotechnology and geochemistry working groups. Additionally, samples were shared with our Icelandic colleague from *matís*.

GEOMAR's short gravity corer (3m, 125mm diameter, 900kg weight) was used at six stations from which a total of about 10m of sediment cores were collected in five successful recoveries (GC in Fig. 5.1, GC01 is not shown on the map). After deployment, the GC was lowered with 1m/s to 50m above seafloor. There, we waited for the corer to stabilize in the water column, which could be monitored by observing the tension on the winch cable. After about 1 – 2min, the

GC was then lowered at speeds between 0.8 – 1.2m/s until ground contact, which is also observable online in the display of the winch tension. After contact, an additional 4 – 5m of slack was given, to allow the GC to fully penetrate into the seafloor. Afterwards, the GC was pulled out of the seafloor with 0.3m/s and, after being completely pulled out, lifted up with 1.0m/s and recovered on deck.

Upon recovery on deck, several parameters (pH, Eh, T) were measured in the material caught in the core catcher using two separate probes (Hach Multimeter MM110DL or HUGER temperature probe). Core catcher and core liner were then removed, the liner was cut into 1m long sections and measurements with the probes were being taken on the bottom and / or top of core sections. After labeling of the core sections, ends were sealed with caps, after which the sections were moved from the deck to the wet lab for further handling. In the lab, the core sections were split lengthwise into working and archive halves using a power disc-saw (Fein-Multimaster) with special attention being paid to not disturb the sediment inside. Both halves were then photographed. Work was continued by taking sub-samples of sediments and pore water from the working halves for microbiology (first) followed by sampling for biotechnology and geochemistry (see following section for additional details for all methods). Finally, both working and archive halves were stored in plastic sleeves within labeled D-tubes. The sections will be deposited at the core repository at GEOMAR.

5.1.3 MUC

Similar to the gravity corer, the objective of sampling with the multi-corer (MUC) was to obtain sediment and pore water samples down to a depth of at maximum 50cm to be analyzed by the geomicrobiology, biotechnology and geochemistry working groups. Additionally, samples were shared with our Icelandic colleague from *matís*. The MUC is equipped with twelve 50cm long plastic liners with diameters of 8cm. It was used at a total of four stations from which three were successfully sampled with sediment cores between 30 – 49cm (MUC in Fig. 5.1, MUC01 is at the same location as GC01 (not on the map), MUC 04 is at the same location as GC05). After recovery, one of the recovered cores upon visual inspection was selected for further processing in the wet-lab.

Fig. 5.3 MUC deployment (June 6th).

5.1.4 BIGO

The BIGO Lander system (Biogeochemical Observatory; Sommer et al. 2009, 2016; see Fig. 5.4) includes two chambers (CHMBR1 and CHMBR2), each equipped with an optode for O_2, conductivity and temperature measurements (Aanderaa), H_2S and STOX sensors (Unisense) as well as a set of optodes with oxygen and temperature sensors monitoring background conditions outside of the chambers during in situ experiments (Fig. 5.5, left). After deployment of the BIGO, the two chambers can be lowered into the sediments for starting the experiments. During the experiments, fluid samples (each 170ml) can be taken directly at predefined points in time, concentrated on a filter (0.2µm pore size) and fixed immediately in situ with RNA shield (Zymo Research) for later lab analyses (Fig. 5.5, middle). Additionally, up to eight syringes (each 50ml) can collect additional water samples from each of the chambers just before the end of the experiments and before retrieving BIGO (Fig. 5.5, right). Just before recovering BIGO, each chamber can be sealed of at the bottom by a slide for sediment collection.

Fig. 5.4 BIGO lander system after recovery.

Fig. 5.5 BIGO sensors for measurements of O_2, conductivity, temperature, H_2S and STOX (left), fluid sampler for RNA fixation (middle), and additional fluid samplers (right).

During this cruise, the BIGO Lander was deployed at two locations, namely at a background site with no or low activity about 60m to the west of the next active vent (BIGO 01) and in close vicinity (<10m) of an active vent covered with anhydrite (BIGO 02; see Fig. 5.1 and a detailed description of the deployments in chapter 5.2.1). Just before recovering BIGO, each chamber was sealed of at the bottom by a slide for sediment collection. After BIGO was retrieved, all sensors were unmounted on deck, data was downloaded, water samples from the chamber and syringes were saved and collected for geochemical and microbial analyses. Additionally, sediment cores (up to 16cm) were collected from the chambers (Fig. 5.6). Sediment cores were then immediately sliced in the laboratory and sub-sampled in a glovebag under oxygen-free conditions for porewater, solid phase and microorganisms. Details for the work carried by the different working groups can be found in the following sub-chapters.

Fig. 5.6 Chamber CHMBR2 after recovery of BIGO 2.

5.2 Geomicrobiology and Biogeochemistry

(Nicole Adam-Beyer, Arlette Wenzel-Storjohann, Mirjam Perner, Wanda Schmitz, Matthias Türk)

5.2.1 BIGO

During the two BIGO deployments (see Fig. 5.1), fluid samples for RNA fixation were scheduled to be collected from each chamber at four points in time (t_0 = 0h, t_1 = 20h, t_2 = 40h, t_3 = 75 – 78h). Additionally, for each chamber three syringes were programmed to collect a total of 150ml of water samples from each of the two chambers just before the end of the experiments.

BIGO 1 deployment: For the first deployment of BIGO on June 6th, our plan was to lower the lander to the seafloor and then follow a traverse to the south of active vent sites in order to find a suitable spot with microbial mats for the deployment. However, with the lander close to the seafloor we could see very little due to the heave of the ship and a poor camera angle, which prevented us from identifying a good patch with indications of hydrothermal activity on the seafloor. In the end the lander was deployed about 60m to the west of the next active vent and left there for a 90h experiment. After recovery of the lander on June 10th, we found out that recovery of water and sediment samples from the chambers as well as sensor data were successful. The fixation device did not add the RNA fixative to the concentrated material on the filters in situ and the Niskin bottles failed to collect a water sample. Two sediment cores showing very similar characteristics were collected, from each chamber one (Fig. 5.7, left). Preliminary sensor data show slightly different degrees of respiration rates for CHMBR1, CHMBR2 and background (Fig. 5.7, right). The temperature in the chambers remained constant during the experiment and unchanged against background water temperature. H_2S and STOX sensor data still need to be assessed.

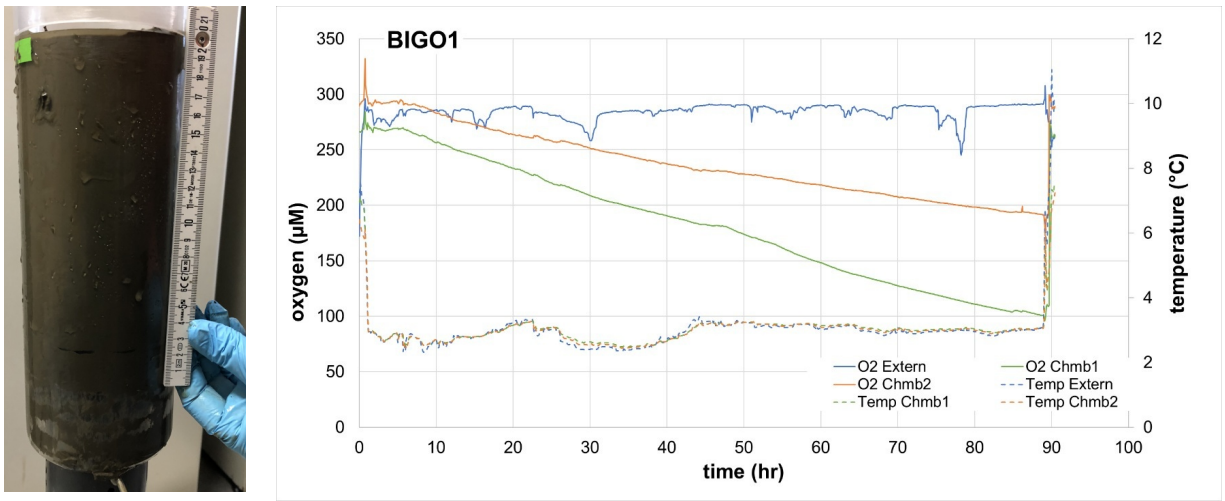

Fig. 5.7 Sediment core collected from chamber 1 after recovery from experiment BIGO 1 (left). The measured sensor data (left) shows time series for O_2 and temperature sensors from the inside of the two chambers and from outside the chambers.

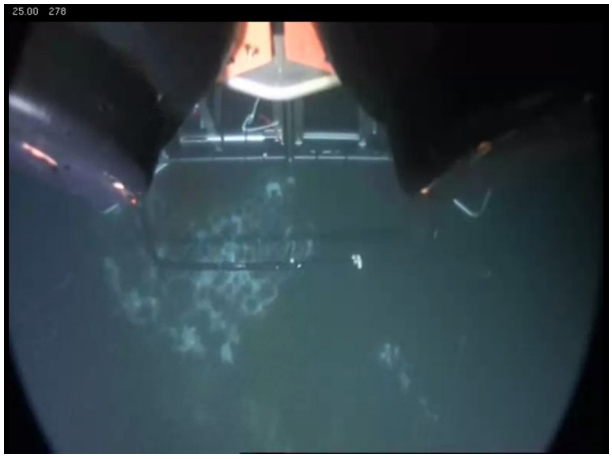

Fig. 5.8 Screenshot of site BIGO 2 moments before deployment of the lander.

BIGO2 deployment: With the new bathymetric map from the AUV dives and adjustments to camera and lighting, we were able to deploy BIGO right on what looked to be a bacterial mat during the second deployment on June 10th.

After Recovery on June 14th, we found out that recovery of water and sediment samples from the chambers as well as sensor data were successful. Also, with some adjustments after the first deployment, the fixation device worked and fixed the samples on filters in situ (except for t2 of chamber 2). The Niskin bottles collected an ambient water sample outside of the experiment. Two sediment cores were collected from each chamber one (Fig. 5.9, left). Preliminary sensor data are shown in Fig. 5.9 (right). CHMBR1 demonstrated oxygen consumption over time where oxygen was depleted in the chamber after 60h. Temperature coincided with background temperature data. CHMBR2 was exposed to temperature increases over time (max 14°C) which came in pulses. In parallel when temperature peaks were monitored, the oxygen optode showed a disturbance in its signature, also in pulses and increasing over time. Likely, warmer gas bubbles emitting from the sediments cause the oxygen optode disturbances and pulsing temperature signals. H_2S and STOX sensor data still need to be assessed.

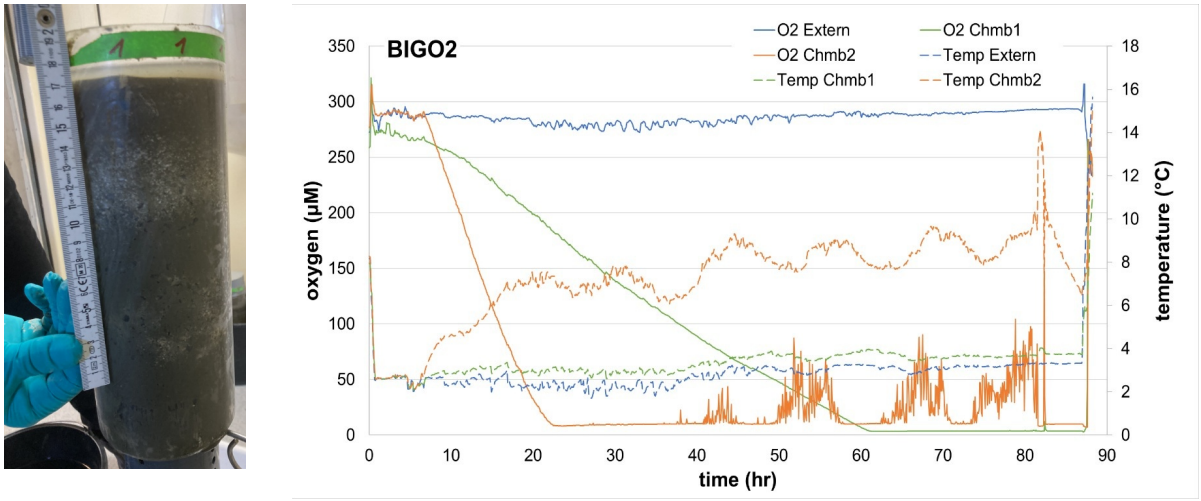

Fig. 5.9 Sediment core collected from chamber 1 after recovery from experiment BIGO 2 (left). The measured sensor data (left) shows time series for O_2 and temperature sensors from the inside of the two chambers and from outside the chambers.

5.2.2 MUC & GC

We collected sediments from two cores from the multi-corer (MUC01 and MUC04), four gravity cores (GC01, GC03, GC04 and GC05) and from the two BIGO deployments. Sediments were sub-sampled and porewaters extracted for later microbial analyses in the home laboratories. For details on collected samples see tables in Appendix (p. 47ff).

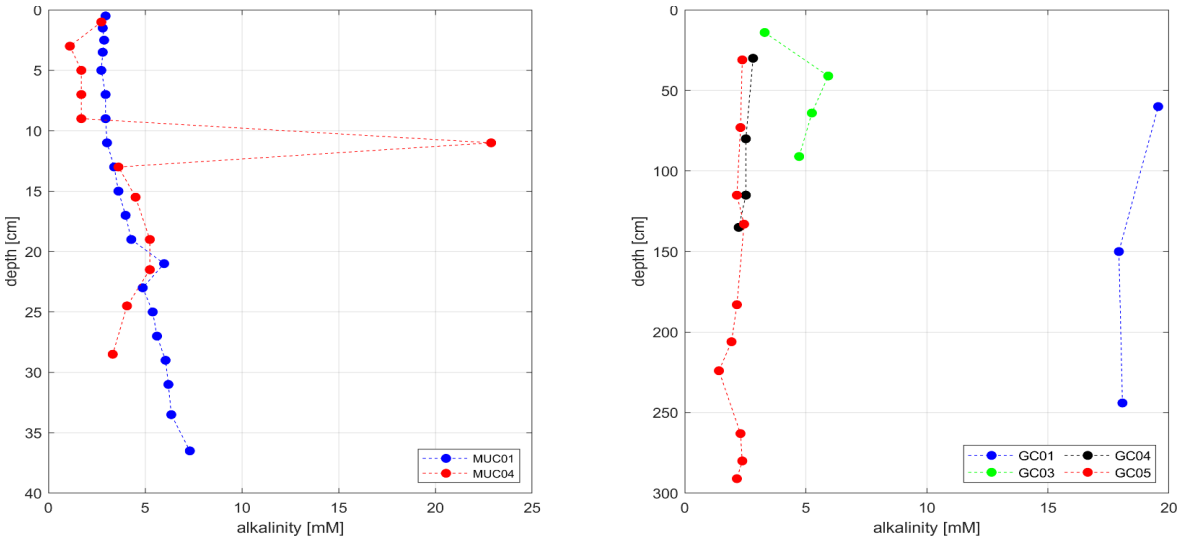

Fig. 5.10 Total alkalinity (TA) from sediments collected with MUC (left) and GC (right). Please note different depth scales. Samples taken at the same site use the same colors (background = blue, active vent = red).

Total alkalinity (TA) and sulfide were the only environmental parameter measured directly on board (TA for BIGO1 sediments by Wanda Schmitz, all other TA and sulfide measurements by Nicole Adam-Beyer). Fig. 5.10 shows the TA measured from MUC (left) and GC (right). TA from the reference cores (MUC1 and GC01, blue lines) were the only samples that showed a considerable TA increase with depth, where at the surface TA of 2mM and in the porewaters of the deepest sediments nearly 20mM were reached (Fig. 5.10). For all other samples, the TA remained mostly below 5mM with the exception of MUC05 (red line, left) where a TA peak was observed at 12 cm just below the sediment horizon, where considerable amounts of gas was emitted during sampling.

The cores collected from the BIGO deployment follow the general trend with relatively homogeneous TA values down to 15 cm depth. However, during each deployment one chamber showed a slight peak in TA (BIGO01_K1 at 9cm → 5mM and BIGO02_K1 at 7cm → 8mM).

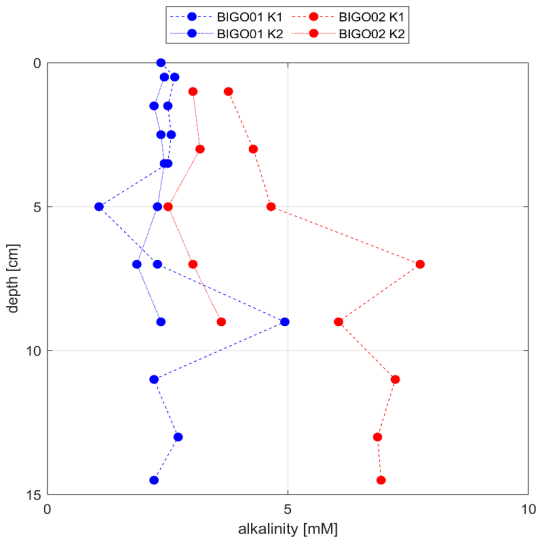

Fig. 5.11 Alkalinity of sediments from the BIGO1 (blue) and BIGO2 deployments (red).

Sulfide concentrations in the sediments from GC01, GC04, GC05, MUC01 and from chambers 1 and 2 of the BIGO01 deployment were below 5µM with maximum depths analyzed at 250 cm (Fig. 5.12). MUC04 reached maximum values of nearly 500µM at 20 cm depth and GC03 peaked with 25µM at ca. 50cm depth (orange and blue lines, respectively, in Fig. 5.12, top). The sediments of chambers 1 and 2 from the BIGO02 deployment reached maximum values of 1mM and 3mM at 15cm and at the surface, respectively (Fig. 5.12, bottom right).

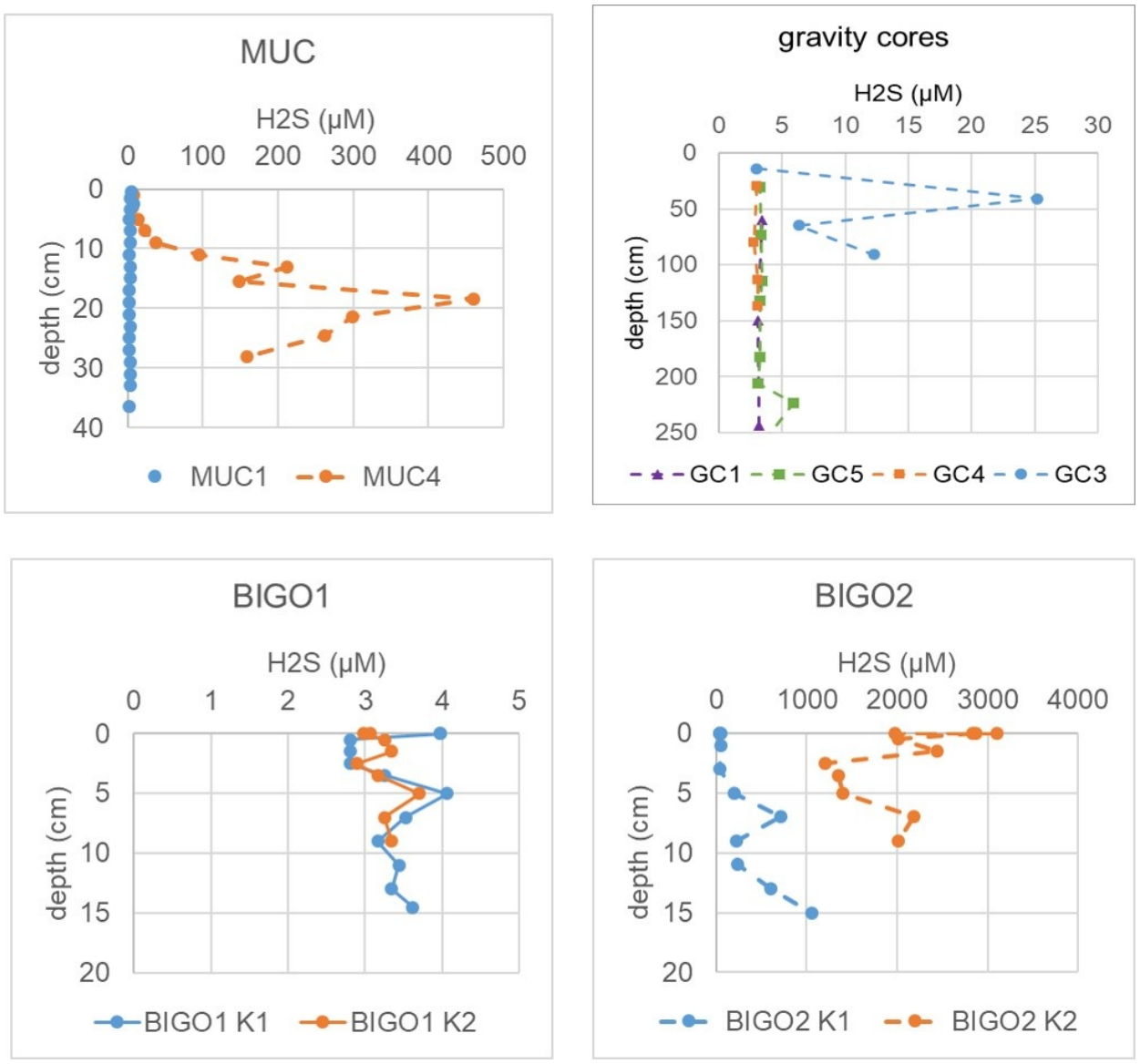

Fig. 5.12 Sulfide measurements for the sediments collected with the MUC, GC and BIGO chambers. Please not the different scales on the plots.

5.3 Marine Natural Product Research

(Arlette Wenzel-Storjohann)

Water samples were collected with a multi-water sampler with attached CTD (see chapter 5.1.1, p. 19). A reference site several km to the west of the vent field was sampled twice (CTD01 & CTD06), all other samples were taken above of in close vicinity to the active vent field (see Fig. 5.1). After recovery on deck, water from the Niskin bottles was directly filled into sterile bottles, filtrated for molecular biological analyses and plated for marine natural product research (see detailed tables of samples in chapter 11.2.2, p. 61) on four different agar media (see below, all amounts per liter) and incubated at room temperature:

Fig. 5.13 MUC sediment cores from MUC01, MUC02 and MUC04 (left to right).

- Marine Broth (MA): Ready-to-use mixture DifcoTM Marine Broth 2216 (37.4g)
- Potato-Dextrose-Agar (PDA): Potato extract (4.0g), Glucose monohydrate (20.0g), Bacto agar (18.0g)
- Tryptic Soy Broth medium 3+10 (TSB3+10): Bacto tryptic soy broth (3g / l), Sodium chloride (10.0g), Bacto agar (18.0 g)
- Wickerham medium (WSP30): Glucose monohydrate (10.0g), peptone from soymeal (5.0g), malt extract (3.0g), yeast extract (3.0g), artificial sea salt (30.0g), Bacto agar (18.0g)

Further processing of the grown bacteria and fungi will take place in the lab at GEOMAR by isolating them, cryo-preservation and identification via Sanger sequencing (bacteria: 16S rRNA gene; fungi: 18S rRNA gene, ITS1).

Additionally, water sample from CTD casts CTD03 (surface, 20m, … every 40m, … 380m), CTD04 (surface, … every 100m, … 380m) and CTD06 (surface, … every 40m, … 400m) and samples from MUC02 and GC03 & GC04 were taken to be analyzed in laboratories at matís (Iceland). On these samples, DNA/RNA will be extracted and – if the RNA is of sufficient quality – will be transcribed that and used for 16S sequencing on the MiSeq Illumina platform. If the RNA is not good enough, sequencing will be performed on the DNA. Additionally, some cultivation of samples from the CTD will be carried out.

Sediment cores from the MUC (see chapter 5.1.3, p.20 and Fig. 5.13) were sliced in different layers and samples were taken for Marine Natural Product research (MNP, see table in chapter 11.2.2, p. 61). For MNP analyses, the sediment samples were diluted with artificial sea water, plated on four different agar media (see above) and incubated at room temperatures. First microbial growth was already observed (Fig. 5.14) and this cultivation will probably yield a few hundred microbial strains. The isolation process will be carried out in the lab as well as the identification of all strains via Sanger sequencing (bacteria: 16S rRNA gene; fungi: 18S rRNA gene, ITS1). In parallel, all isolates will be cryo-preserved and – as future perspective – the most promising bacterial and fungal strains could be re-cultivated later in order to test their bioactivity potential (e.g. antibacterial, antitumoral activity) and elucidate their metabolic potential via UPLC-Q-TOF-MS (ultra-high performance liquid chromatography with quadrupole time-of-flight mass spectr.).

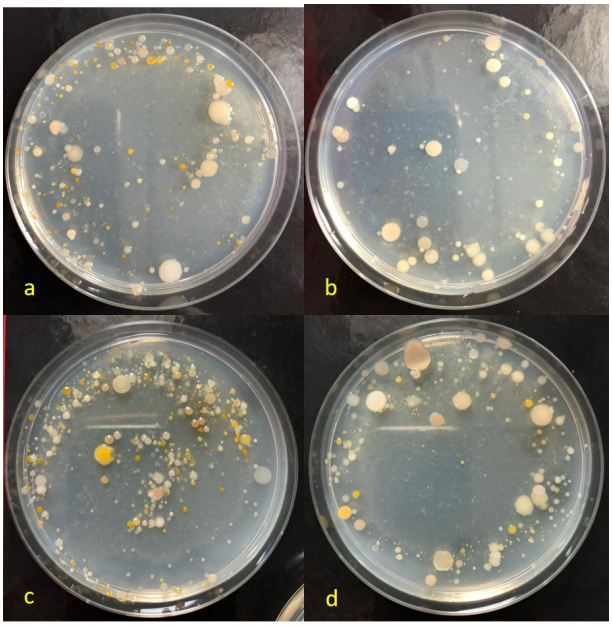

Fig. 5.14 Marine agar plates inoculated with sediment samples from Multicorer after 8 days incubation at room temperature, a: MUC01 soft layer above sediment, b: MUC01 0 – 1 cm layer, c: MUC02 soft layer above sediment, d: MUC02 0 – 1 cm

5.4 Geochemistry

(Wanda Schmitz)

Several cm³ of sediment and pore water fluids were recovered for geochemical studies. Geochemical analyses will be carried out at GEOMAR. All sampling tools and instruments were free of metal to avoid contamination regarding trace metal analyses.

The sediment samples were taken from the center of the working halves of gravity cores and from slices of the MUC cores. Whenever possible, sediment and pore water were recovered within the same depth interval of samples taken for microbiological analyses. Cut-off, tip-less syringes of 20ml were used for collecting sediment samples, which were stored in labeled zip-lock plastic bags. Sediment samples for mercury analyses were taken via 3ml tip-less syringes and then transferred to PP mini vials, which were stored in two zip-lock plastic bags to avoid cross contamination of samples. The core halves were also analyzed for pH, Eh and temperature (Hach Multimeter MM110DL). In total 38 samples were retrieved for subsequent analysis.

After taking the sediment samples, pore water fluids were collected on the working half using Rhizon CSS (Core Solution Samplers). They consists of a 4cm porous polymer tube (0.15µm) with a flat tip and a diameter of 2.5mm, supported by a glass fiber strengthener and connected with a PEC/PVC tubing of 12cm and female Luer Lock (LL). The syringes (20ml) were screwed directly on the LL and pistons were kept in place with retainers (wooden pieces) that enabled a vacuum to be created (Rhizosphere Research Products, 2018). The pore fluids were stored in

20ml, acid-cleaned, PP mini vials. For ICP-OES and dissolved trace metal analyses (DTM) preparation, 3ml of the collected pore fluid was transferred into an acid-cleaned, 3ml PP vial and acidified by adding 2.4µl of q-HCl (32%) per ml sample. For mercury solution analyses, 1-2 ml of pore fluid was transferred into a 2ml PP vial and then acidified by adding 4µl of q-HCl (32%) per ml pore fluid. 2-3 ml of pore fluid was transferred into 4ml PP vials and stored at -80°C for nutrient analyses. A total of 108 pore water fluid samples were collected.

5.5 AUV

(Anna Jäkle, Patrick Leibold, Nikolaj Diller, Torge Kurbjuhn, Danilo Scheppukat)

5.5.1 Instrumentation

Anton and *Luise* are configurable autonomous underwater vehicles (AUV) of the type Girona 500, which are designed to operate at a maximum depth of 500m. Three torpedo-shaped hulls (0.3m diameter, 1.5m length, lower one not installed during dives at GVF) held together by an aluminum frame, provide a good hydrodynamic performance and offer sufficient space for five thrusters, an advanced integrated navigation system, several means for communication and sensor payloads. The overall dimensions of the vehicle are 1m in height, 1m in width, 1.5m in length and a weight of less than 200kg. The two upper hulls, which contain the buoyancy foam and the electronics housing, are positively buoyant, while the lower one contains heavier elements such as the batteries and the payload. This particular arrangement of components makes the separation between the center of gravity and the center of buoyancy about 11cm, which is significantly more than any typical torpedo shape design. This provides passive stability in pitch and roll even at low speeds, making it suitable for imaging surveys. Another advantage is the capability to be easily reconfigurable for different tasks.

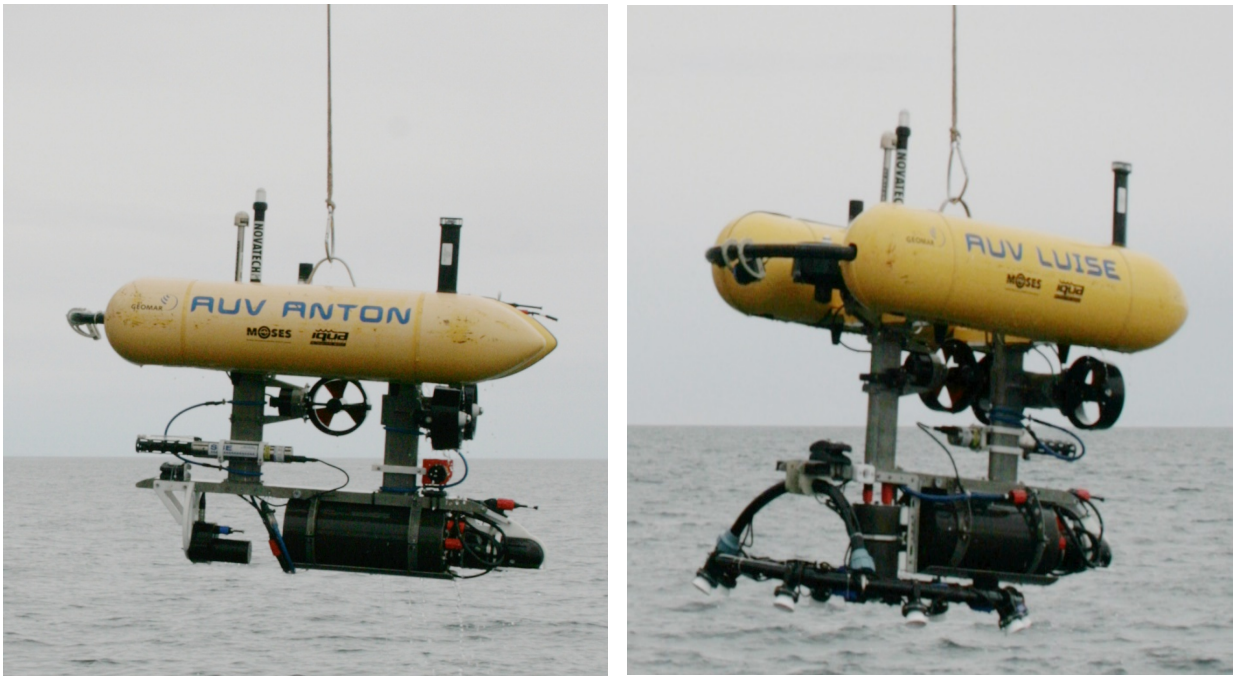

Fig. 5.15 AUV Anton with attached multibeam system (left) and AUV Luise with attached camera and LEDs.

The COLA2 infrastructure on the Girona 500 AUVs is the central control software, developed by IQUA Robotics (Girona, Spain). The communication under and above water is controlled by BEL-

UGA, which will be described later in detail. The BELUGA software is developed by the AUV group at GEOMAR.

In addition to the navigational sensors like INS (Inertial Navigation System), DVL (Doppler Velocity Log), Pressure Sensor, USBL and GPS, a CTD (Conductivity, Temperature, Depth) type Seabird FastCAT SBE49 is mounted by default. An overview of all components for navigation and optional payload can be found in the following table:

Tab. 5.1 Technical specifications of AUVs Anton & Luise.

System	Device	Description
Navigation	iXblue Phins Combat C3	The internal navigation (INS) unit processes sensor data and provides position information. The error of this INS is 0.15° for heading and 0.05° for roll and pitch. This leads to a 0.3% position accuracy.
	Teledyne RDI Explorer 600kHz	The DVL measures altitude and velocity relative to the sea floor.
	Valeport ultraP	The sensor measures the pressure and converts it to water depth.
	USBL: Evologics S2CR 18/34	Modem combining underwater communication and USBL positioning, thus, enabling vehicle's integration into the BELUGA network.
	Quectel l86 GNSS module	The GPS is used to determine the absolute position at the surface.
	Tritech Gemini 720im	Multibeam imaging sonar in a compact housing with depth rating of 750 m. Mounted forward-looking at top edge of AUVs as a preparation of obstacle avoidance. Optional on AUV *Luise a*nd AUV *Anton*.
Payload	Sea-Bird SBE 49 FastCAT	Measurement of conductivity, temperature and pressure to derive sound velocity. Payload on AUV *Anton* and AUV *Luise*.
	CoraMo mk II Camera	Down- or forward-looking camera system for photographic surveys, built by the AUV team of GEOMAR. It can take up to two images per second with a resolution of 12.34 MP. CoraMo supports connections for eight high power LEDs that are arranged in a ring around the camera. Optional payload on AUV *Anton* and AUV *Luise*.
	Norbit Wideband Multibeam Sonar WBMS	Wideband multibeam sonar for high resolution bathymetry with flexible swath coverage of 5 – 210° and 256 – 512 beams. The nominal operating frequency is 400 kHz (frequency agility 200 – 700 kHz) with an adaptive ping rate of up to 60 Hz. Optional payload on AUV *Anton*.
	Fluorometer Seabird ECO FLNTURTD	Chlorophyll and turbidity sensor with 6000 m depth rating. Fluorescence is measured with an excitation wavelength of 470nm, an emission wavelength of 695nm and a typical range of 0 to 50µg/l Chl. Turbidity is measured with a wavelength of 700nm and a sensitivity of 0.013NTU. The sample rate of up to 8Hz is user selectable. Optional payload on AUV *Anton* and AUV *Luise*.
	Sensys MX3D UW	System with up to five single magnetometers connected to one data acquisition unit. Each 3-component fluxgate magnetometer is sampled at 200Hz. Due to problems with AUV *Luise* towards the end of the cruise, the magnetometers were not used.

Missions can have a duration of up to 9 hours and a total length of about 10km, depending on settings, payload and environmental conditions like currents and diving depth. The maximum

speed is 1m/s while the minimum speed is not limited, even hovering at one point for an arbitrary amount of time is possible.

For this cruise, measurement time was limited to about 6h, which left about 4.5 – 5h of operation on the seafloor. AUV *Anton* was equipped with a Norbit Wideband Multibeam Sonar WBMS with an operating frequency of 400kHz, gain settings of 20 and 40 for the first and second dive, respectively, a swath coverage of 130°, and an automatic ranging mode. For the multibeam missions the distance to the ground was set to 20m, which ensured a stable DVL lock onto the seafloor. Profile lines were planned with a spacing of 50m and a speed of 0.5m/s.

AUV Luise was equipped with a CoraMo mk II camera and eight high power LEDs to take pictures for photogrammetric surveys over selected targets. The images and the corresponding metadata can be found in the missions "pictures" directory. A file containing information about parameter settings of the camera and the CoraMo system in total as well as navigational and environmental information (e.g. position and temperature) is written for each file. Additionally, one file containing each single CSV (comma separated values) files data line is created after a dive (images_metadata.csv) and can also be found in the pictures directory. Depending on the settings, a second file with metadata (metadata_information.csv) is written during the dive. It contains some information about camera and system parameters and focuses more on the information needed to build mosaics from the images like position, rotation and general information about the camera equipment.

The core of the transponders used at GEOMAR is a modified S2C 18/34 Evologics modem with buoyancy foam. In addition to the default version of the modem, the transponders are equipped with a wake-up module, a pressure sensor and a mechanical release that can be queried and triggered by acoustic commands from the surface. An internal computer allows the development of dedicated software running directly on the transponders. During AUV missions, the transponders were placed in a triangle of approx. 700m edge length and 10m above ground.

The BELUGA system was used during this cruise to monitor and control both AUV platforms and LBL transponders in real time. BELUGA handles all communication with surface and underwater platforms by automatically selecting the optimal communication channel. By instantly visualizing incoming data from the platforms, operators onboard the vessel could immediately react to events or anomalies. Positions of all integrated platforms are estimated using an Evologics USBL topside unit and displayed in the map of the BELUGA front-end to allow for an overview of the entire situation. Customized dashboards offer different options depending on the platform. This allows the visualization of specific information as well as a selection of customized actions to control the platform. In addition to displaying the last transmitted data of a platform, each parameter can be also displayed in a graph over time. External data, such as remote sensing or model data can be integrated into the map.

Supported by the BELUGA system, downloading and processing of raw sensor data from dives can also be automated. The data is processed according to standards and formats in coordination with the data management team. A report of the exported mission with summarized information is also created.

5.5.2 Deployments

When operating the AUVs in different environments or after a change in payload configuration, the trim and buoyancy have to be adjusted. Due to higher salinity in the working area offshore Iceland in comparison to the Baltic Sea, buoyancy foam was removed. To check the trim while diving, a short dive (*Anton280*) in 10m depth was conducted shortly after arriving in the working area. With the adjusted buoyancy, the trim was found to be sufficiently balanced to directly continue with dive *Anton281*, a first dive to 380m depth while supporting the navigation unit of the vehicle via USBL on its way down to check at what altitude above seafloor its DVL (Doppler Velocity Log) gets bottom lock. Stable locks were obtained at altitudes of roughly 20m above seafloor, which was consequently chosen as operating altitude for all following missions with *Anton* (see Fig. 5.16 for an overview of tracks flown with Anton in the main working area).

Dive *Anton282* was a first test to estimate optimal parameters for multibeam missions. The dive had to be aborted after the descent to 380m due to a wrong setting in the safety altitude. After correction, the mission was restarted as dive *Anton283.* A flight altitude of 20m above ground and a line spacing of 50m of adjacent track lines with a swath width of 130° provided sufficient overlap between for the automatic generation of bathymetric maps. With the data acquired in the following 2:47h, a first map of 650m x 250m covering the central section of the

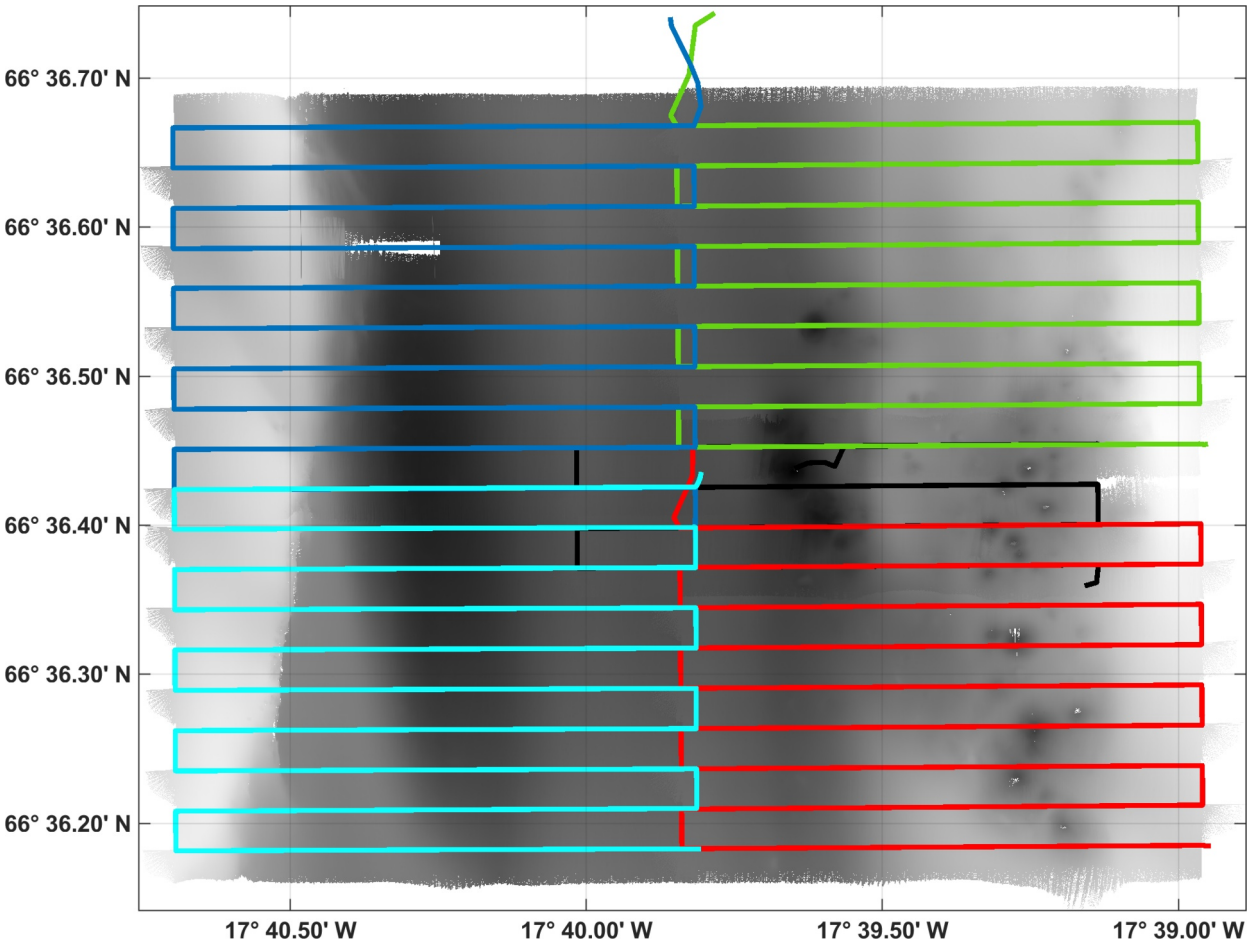

Fig. 5.16 Track planning of missions with AUV Anton in the main working area around the active vent field. Lines show the tracks for dives 283 (black), 284 (red), 286 (green), 287 (blue) and 288 (cyan). In the background, the acquired bathymetric data are displayed as gray-shaded images.

hydrothermal vent field with a horizontal resolution of approximately 40 cm x 40 cm was generated in post-processing. The following missions covered the areas around this first patch. Dive *Anton284* covered the southern part of the Grimsey Vent Field. While performing the pre-dive routine, one of the thrusters did not work and was replaced by one of AUV *Luise's* Thrusters. With two hours delay, the dive was started and successfully finished. Dive *Anton285* had to be started again due to wrong altitude/depth settings for the first descent. The next attempt, listed as *Anton286*, covered the northern part of the Grimsey Vent Field. Acquisitions in the main working area were completed with dives *Anton287* and *Anton288*, which covered the area to the West of the vent field also yielding a detailed insight into the normal fault, which is of interest for the geological interpretation of the working area. The final dive *Anton289* explored an area of 440m x 420m several kilometers to the NE of the Grimsey Vent Field. An overview of the acquired data is shown in Fig. 5.17 (p. 34).

With each patch in the main working area, an area of approx. 650m x 520m was surveyed. Within each patch, tracks were flown along east ↔ west profile lines with a line spacing of 50m. Overlaps between adjacent patches are about 20m. A merged map of all individual patches into a single map covers an area of approximately 1200m x 980m or 1.2km^2.

Photo missions were carried out with AUV *Luise*. Dive *Luise299* was carried out to determine the optimal altitude above the seafloor for photo missions. Altitudes of 4.6m, 3.6m, 3.1m, 2.6m and 2.4m were tried. These altitudes refer to the center of the AUV, the camera in the dome-port is located 60cm below. An altitude of 2.6m was determined to be optimal in terms of allowing for a safe operation while still producing well illuminated images. Further settings of this mission were 0.3m/s speed, a line spacing of 1.5m and a waypoint tolerance of 2m as no photo mosaic was to be produced from this first test dive. With these settings, it was clear that a generation of mosaics across the active chimney structures would not be possible, because their flanks where too steep. Based on the detailed multibeam map generated from dive *Anton284*, three suitable structures were identified to the W and SW of the central active vent sites and covered with N ↔ S profiles during dive *Luise300*. By post-processing with *AgiSoft MetaShape*, three photo-mosaics including digital elevation models were produced. Each patch covers an area of 30m x 30m. Images were also taken on the transits between the three targets. Dive *Luise301* was scheduled to cover a structure just to the N of the structures covered during the previous dives. However, due to problems in the acoustic communication the vehicle lost orientation during the descent. A connection via acoustic communication or WiFi could not be established again. Luckily, the vehicle was visually detected after a 20h long search mission with empty batteries, drifting at the surface. The last mission *Luise302* delivered two photo-mosaics, one at the location of BIGO01 and a structure just N of this landing site. The photo-mosaics each cover an area of about 35m x 35m and were performed with the same settings as the ones used during the previous dives.

5.5.3 Preliminary Results

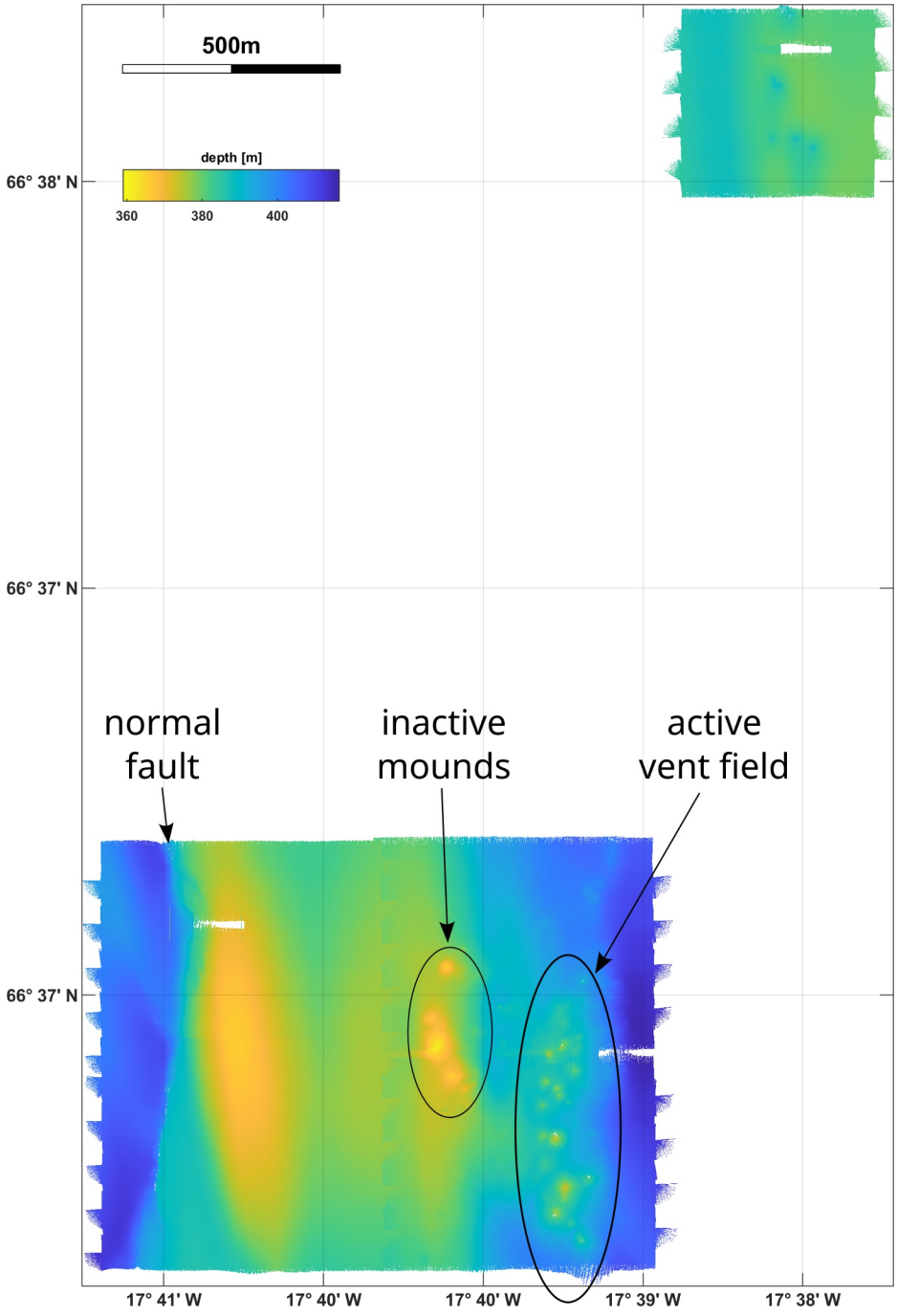

Fig. 5.17 Overview map of multibeam data acquired with AUV Anton. The map of the main working are in the SW consists of individual patches from the first five dives. During the last dive, an area about 3km to the NW was surveyed, where samples were taken during previous cruises. Please note that no shifts or corrections / interpolations to remove outliers / missing data were applied in the creation of this map.

The above map gives a first impression of the coverage of bathymetric data acquired with AUV *Anton* during the cruise. The main work was carried out to cover an area including the active vent field, some hydrothermal mounds adjacent to the W of the active field with no or very little activity, and finally a prominent escarpment further to the W which most likely is connected to a normal fault. All maps are displayed without any further processing or corrections applied. Due

to the fact that the inactive mounds are higher up in the bathymetry (i.e. at shallower depth), they appear more prominent in the above map. Thus, the above map is only intended to give a general overview of the acquired data.

Fig. 5.18 shows a zoomed section of the same data, here in a 3D view as illuminated surface. Two large and one smaller mound are fully encompassed, additional mounds are cut off at the edges of the displayed surface. On top of the two larger mounds needle like structures show that the horizontal resolution of the acquired data is high enough to map out the slim chimney structures on top of the mound. The illuminated surface shows a pattern of N ↔ S striking stripes, which are perpendicular to the flight direction of the AUV during acquisition. These patterns are evident in most of the acquired datasets and will need to be addressed in a more thorough post-processing to be carried out after the cruise. It should be clearly stated that in the current form with just the standard processing steps being applied onboard directly after recovery of the AUV, the results are already pretty stunning and have the potential to yield great insights into the geological structure of the vent field.

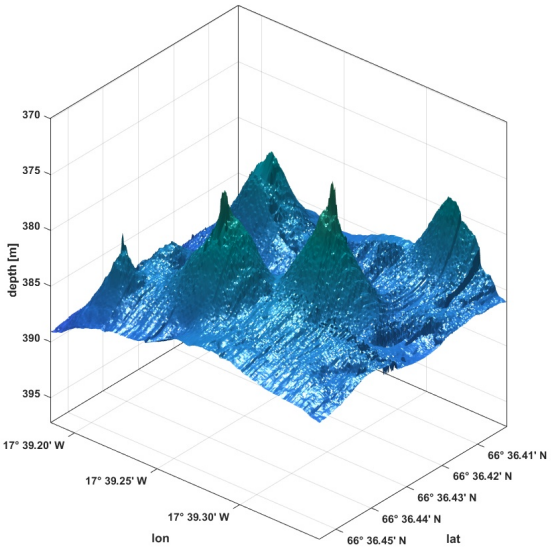

Fig. 5.18 Illuminated 3D view of a subset of the newly acquired bathymetric data.

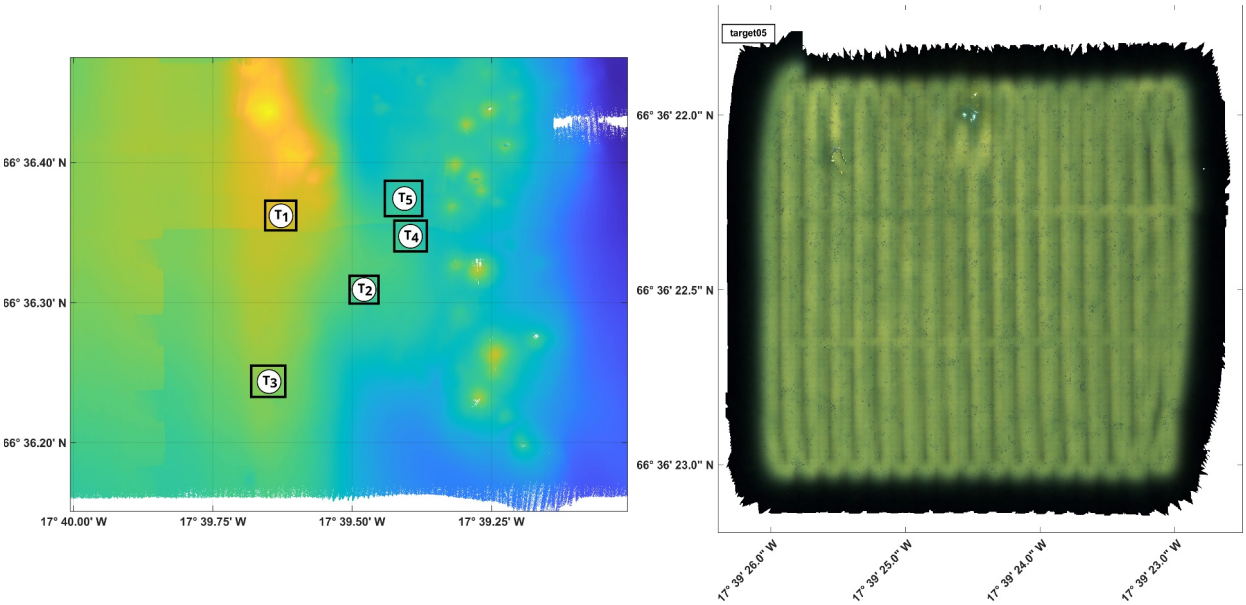

Fig. 5.19 Overview map showing locations of photo-mosaics taken with AUV Luise (left). The photo-mosaic of target05 (right), shows a vertical stripe pattern (evident in all mosaics), an acquisition artifact to be handled in post-processing. All mosaics can be found in the appendix (chapter 11.3, p. 66ff).

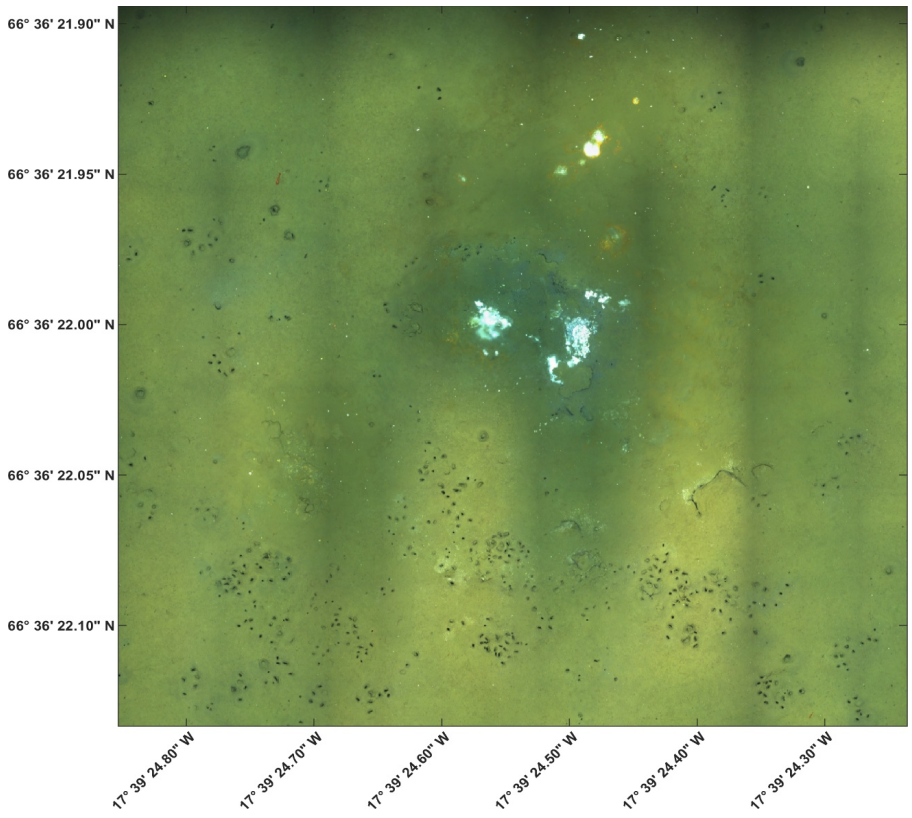

Fig. 5.20 Zoom into northern section of photo-mosaic of target T5 (area ca. 8m x 8m, resolution ca. 5mm).

As AUV *Luise* had to be operated close to the seafloor (2.6m), investigations of the mound structures were not considered to be a safe option. Instead, focus was put on several small depressions resp. small mound structures between the active and inactive mounds (targets T2, T4 and T5 in Fig. 5.19, left) and to the south of the inactive mound (targets T1 and T3 in Fig. 5.19, left). Plans to also survey the normal fault to the west on the last days of the cruise, were canceled after *Luise* was nearly lost and further operation was deemed to be unsafe due to the unstable communication to the AUV. As an example, Fig. 5.19 (right) shows the photo-mosaic of target T5, which was stitched together from a total of 4900 single images. Depending on the size of the targets, 3600 – 5100 single images were used. The vertical stripe pattern – evident similarly in all mosaics – which is an acquisition artifact due to the fading illumination toward the edge of the single pictures and needs to be addressed in post-processing.

Fig. 5.20 shows details of the northern section of the photo-mosaic displayed in Fig. 5.19 (right) with white patches (anhydrite ?!) surrounded by many small holes in the seafloor. When zooming further into the patches, they have a somewhat blurry appearance which could be an indication of active fluid venting from the seafloor. It will be interesting to integrate the CTD data, which was acquired at the same time on AUV *Luise*, to see if any temperature anomaly is evident in the water column above these patches. Also, the integration with the local digital elevation model derived as part of the stitching process will yield further leads for a structural interpretation. The picture displayed here has a resolution of about 5mm, but higher resolution of up to 1mm are also available. However, at such high resolutions, the resulting mosaic-images of targets have sizes of up to 4Gb and, thus, require graphic cards with sufficient memory.

6 Station List AL595

6.1 Overall Station List

Tab. 6.1 Overall station list.

Station AL595	Device	Event Time	Latitude	Longitude	Depth [m]	Action / Comment
1-1	CTD water	05.06.23 13:25	66° 36,358' N	17° 41,604' W	399	in the water
1-1	CTD water	05.06.23 13:53	66° 36,345' N	17° 41,718' W	5	on deck
2-1	AUV Anton	05.06.23 14:03	66° 36,294' N	17° 41,726' W	379	at surface
2-1	AUV Anton	05.06.23 14:06	66° 36,288' N	17° 41,729' W	6	on deck
2-1	AUV Anton	05.06.23 14:10	66° 36,283' N	17° 41,747' W	45	in the water
2-1	AUV Anton	05.06.23 15:26	66° 36,242' N	17° 41,641' W	399	on deck
3-1	AUV Luise	05.06.23 15:34	66° 36,249' N	17° 41,649' W	399	at surface
3-1	AUV Luise	05.06.23 15:36	66° 36,249' N	17° 41,642' W	399	on deck
4-1	MUC	06.06.23 06:19	66° 36,401' N	17° 41,473' W	395	in the water
4-1	MUC	06.06.23 06:47	66° 36,414' N	17° 41,496' W	395	on deck
5-1	CTD water	06.06.23 07:48	66° 36,311' N	17° 39,264' W	367	in the water
5-1	CTD water	06.06.23 08:16	66° 36,333' N	17° 39,380' W	375	on deck
6-1	BIGO	06.06.23 13:40	66° 36,248' N	17° 39,058' W	387	in the water
6-1	BIGO	06.06.23 14:42	66° 36,367' N	17° 39,418' W	379	deployed
7-1	Transponder	07.06.23 06:09	66° 36,530' N	17° 39,963' W	373	deployed
7-2	Transponder	07.06.23 06:31	66° 36,082' N	17° 40,384' W	382	deployed
7-2	Transponder	07.06.23 06:45	66° 36,115' N	17° 40,441' W	381	released
7-2	Transponder	07.06.23 06:49	66° 36,114' N	17° 40,403' W	381	at surface
7-2	Transponder	07.06.23 06:53	66° 36,038' N	17° 40,405' W	382	on deck
7-2	Transponder	07.06.23 07:01	66° 36,086' N	17° 40,364' W	382	deployed
8-1	AUV Anton	07.06.23 08:11	66° 36,525' N	17° 39,638' W	360	in the water
7-3	Transponder	07.06.23 10:24	66° 36,086' N	17° 39,539' W	378	deployed
8-1	AUV Anton	07.06.23 12:06	66° 36,344' N	17° 39,094' W	390	on deck
9-1	GC	07.06.23 12:32	66° 36,398' N	17° 41,503' W	396	in the water
9-1	GC	07.06.23 12:54	66° 36,395' N	17° 41,484' W	396	on deck
10-1	CTD water	08.06.23 06:20	66° 36,452' N	17° 39,339' W	379	in the water
10-1	CTD water	08.06.23 06:55	66° 36,466' N	17° 39,274' W	377	on deck
11-1	MUC	08.06.23 07:07	66° 36,435' N	17° 39,316' W	372	in the water
11-1	MUC	08.06.23 07:30	66° 36,439' N	17° 39,236' W	374	on deck
12-1	AUV Luise	08.06.23 08:04	66° 36,444' N	17° 39,692' W	354	in the water
12-1	AUV Luise	08.06.23 09:23	66° 36,442' N	17° 39,644' W	354	on deck
13-1	GC	08.06.23 11:16	66° 36,411' N	17° 39,263' W	376	in the water
13-1	GC	08.06.23 11:35	66° 36,411' N	17° 39,263' W	378	on deck
13-2	GC	08.06.23 12:21	66° 36,420' N	17° 39,271' W	376	in the water
13-2	GC	08.06.23 12:37	66° 36,417' N	17° 39,268' W	378	on deck,15m shift
14-1	AUV Anton	08.06.23 13:13	66° 36,456' N	17° 39,787' W	371	in the water

7-1	Transponder	08.06.23 14:00	66° 36,528' N	17° 39,980' W	374	on deck
7-2	Transponder	08.06.23 14:21	66° 36,071' N	17° 40,375' W	384	on deck
7-3	Transponder	08.06.23 14:41	66° 36,076' N	17° 39,510' W	382	on deck
14-1	AUV Anton	08.06.23 17:59	66° 36,040' N	17° 39,301' W	389	on deck
15-1	Transponder	09.06.23 07:00	66° 36,743' N	17° 39,996' W	377	deployed
15-2	Transponder	09.06.23 07:18	66° 36,752' N	17° 39,690' W	376	deployed
16-1	AUV Anton	09.06.23 07:36	66° 36,758' N	17° 39,745' W	377	in the water
17-1	AUV Luise	09.06.23 10:17	66° 36,384' N	17° 39,625' W	377	in the water
16-1	AUV Anton	09.06.23 12:41	66° 36,484' N	17° 38,932' W	377	on deck
18-1	CTD water	09.06.23 12:53	66° 36,386' N	17° 39,643' W	377	in the water
18-1	CTD water	09.06.23 13:25	66° 36,383' N	17° 39,583' W	364	on deck
19-1	MUC	09.06.23 13:38	66° 36,369' N	17° 39,614' W	367	in the water
19-1	MUC	09.06.23 14:07	66° 36,394' N	17° 39,601' W	360	on deck
17-1	AUV Luise	09.06.23 14:33	66° 36,141' N	17° 39,360' W	391	on deck
20-1	GC	09.06.23 15:05	66° 36,367' N	17° 39,595' W	366	in the water
20-1	GC	09.06.23 15:25	66° 36,359' N	17° 39,618' W	366	on deck
21-1	CTD water	09.06.23 16:09	66° 36,292' N	17° 39,188' W	382	in the water
21-1	CTD water	09.06.23 16:32	66° 36,290' N	17° 39,244' W	378	on deck
6-1	BIGO	10.06.23 05:55	66° 36,345' N	17° 38,972' W	403	on deck
22-1	AUV Anton	10.06.23 07:20	66° 36,697' N	17° 39,852' W	382	in the water
23-1	AUV Luise	10.06.23 10:14	66° 36,444' N	17° 39,260' W	382	in the water
22-1	AUV Anton	10.06.23 12:09	66° 36,374' N	17° 39,861' W	382	on deck
15-2	Transponder	10.06.23 14:21	66° 36,738' N	17° 39,752' W	382	on deck
15-1	Transponder	10.06.23 14:34	66° 36,724' N	17° 40,015' W	382	on deck
24-1	BIGO	10.06.23 18:48	66° 35,990' N	17° 34,841' W	382	in the water
24-1	BIGO	10.06.23 20:01	66° 36,390' N	17° 39,220' W	375	deployed
23-1	AUV Luise	11.06.23 07:48	66° 34,102' N	17° 35,252' W	297	on deck
25-1	CTD water	11.06.23 09:48	66° 36,368' N	17° 41,607' W	398	in the water
25-1	CTD water	11.06.23 10:21	66° 36,313' N	17° 41,490' W	398	on deck
26-1	AUV Luise	13.06.23 07:59	66° 36,302' N	17° 39,419' W	376	in the water
27-1	CTD water	13.06.23 09:40	66° 36,387' N	17° 39,309' W	377	in the water
27-1	CTD water	13.06.23 10:02	66° 36,350' N	17° 39,342' W	378	on deck
28-1	MUC	13.06.23 10:21	66° 36,381' N	17° 39,293' W	373	in the water
28-1	MUC	13.06.23 10:43	66° 36,380' N	17° 39,299' W	373	on deck
29-1	GC	13.06.23 11:00	66° 36,382' N	17° 39,306' W	373	in the water
29-1	GC	13.06.23 11:20	66° 36,384' N	17° 39,279' W	372	on deck
26-1	AUV Luise	13.06.23 12:16	66° 36,373' N	17° 38,871' W	404	on deck
30-1	AUV Anton	13.06.23 12:32	66° 36,414' N	17° 39,772' W	370	in the water
30-1	AUV Anton	13.06.23 17:18	66° 36,143' N	17° 39,775' W	378	on deck
31-1	AUV Anton	14.06.23 06:13	66° 37,404' N	17° 38,861' W	378	in the water
31-1	AUV Anton	14.06.23 09:26	66° 37,695' N	17° 38,989' W	383	on deck
24-1	BIGO	14.06.23 10:34	66° 36,296' N	17° 39,248' W	383	on deck
32-1	GC	14.06.23 13:12	66° 36,463' N	17° 40,540' W	383	in the water
32-1	GC	14.06.23 13:28	66° 36,467' N	17° 40,529' W	383	on deck

6.2 Individual Station Lists

6.2.1 CTD

Tab. 6.2 Individual station list of CTD casts during cruise AL595.

Station AL595	CTD	Latitude	Longitude	Depth [m]	Comment
1-1	CTD01	66° 36,358' N	17° 41,604' W	399	Background location, bottom-water only Water also used for calibration of BIGO sensors same location as GC01 and MUC01
5-1	CTD02	66° 36,311' N	17° 39,264' W	367	Sampling at site BIGO01, bottom-water only
10-1	CTD03	66° 36,452' N	17° 39,339' W	379	Sampling of water column (every 40m) at site MUC02, which is located ca. 50m to the NW of the active vent field
18-1	CTD04	66° 36,386' N	17° 39,643' W	377	Sampling in water column (every 100m) above small depression, same site as GC04, MUC03 (no recovery), also visited by AUV Luise for photo-mosaic
21-1	CTD05	66° 36,292' N	17° 39,188' W	382	Sampling of bottom-water only location south of active vent field
25-1	CTD06	66° 36,368' N	17° 41,607' W	398	Same site as CTD01 sampling of water column (every 40m)
27-1	CTD07	66° 36,387' N	17° 39,309' W	377	Sampling of bottom-water only in center of southern active vent field Same location as MUC04 and GC05.

6.2.2 Gravity Core

Tab. 6.3 Individual station list of gravity core locations during cruise AL595.

Station AL595	GC	Latitude	Longitude	Depth [m]	Recovery [cm]	Comment
9-1	GC01	66° 36,398' N	17° 41,503' W	396	300	Background (homog. non-indurated greenish gray clay). T_{bottom} = 5.1°C. Same location as MUC01, CTD01 & CTD06
13-1	GC02	66° 36,411' N	17° 39,263' W	376	90	Only temperature measured (T_{bottom} = 30.8°C), no samples taken. Immediately moved on to GCO3.
13-2	GC03	66° 36,417' N	17° 39,268' W	378	99	Greenish gray sand size anhydrite/talc grains interlaid with coarse anhydrite sand layers. T_{bottom} = 81.9°C

Station AL595	GC	Latitude	Longitude	Depth [m]	Recovery [cm]	Comment
20-1	GC04	66° 36,367' N	17° 39,595' W	366	158	Homogeneous dark greenish brown silt/clay with intercalation of sand size anhydrite. Dehydrated very hard dark brown clay layer. T_{bottom}: 10.6°C Same location as MUC03 (no recovery).
29-1	GC05	66° 36,382' N	17° 39,306' W	373	300	Grayish white sand size anhydrite/talc grains interlaid with coarse anhydrite sand layers. T_{bottom} = 84.1°C Same location as MUC04 and CTD07.
32-1	GC06	66° 36,463' N	17° 40,540' W	383	60	Background sediment composed of homogeneous non-indurated greenish gray clay. T_{bottom} = 5.9°C

6.2.3 MUC

Tab. 6.4 Individual station list of locations of multi-corer (MUC) during cruise AL595 with sediment descriptions.

Station AL595	MUC	Latitude	Longitude	Depth [m]	Recovery [cm]	Comment
4-1	MUC01	66° 36,401' N	17° 41,473' W	395	46 (Liner 1) 48 (Liner 2)	Background site ca. 3Km to W of vent field. Homogeneous, fine, (dark) brownish material, becoming more dry and clayey with depth, empty tubes and Polychaeta in the first few cm
11-1	MUC02	66° 36,435' N	17° 39,316' W	372	49 (Liner 1)	Ca. 50m NW of active vent field, fine brownish to dark brownish material, becoming more dry and clayey with depth, empty tubes and Polychaeta in the first few cm
19-1	MUC03	66° 36,369' N	17° 39,614' W	367	0	Winch cable entangled in MUC
28-1	MUC04	66° 36,381' N	17° 39,293' W	373	30 (Liner 1) 30 (Liner 2)	Close to active vent, dark brownish sediment interrupted with coarser white layers, H2S smell and strong degassing (CO_2?)

6.2.4 BIGO

Tab. 6.5 Individual station list of BIGO locations during cruise AL595.

Station AL595	BIGO	Latitude	Longitude	Depth [m]	Comment
6-1	BIGO01	66° 36,367' N	17° 39,418' W	379	Background location
24-1	BIGO02	66° 36,390' N	17° 39,220' W	375	Directly south of active mound, one chamber directly on white patch.

6.2.5 AUV

Tab. 6.6 Table of dives carried out with AUV Anton and AUV Luise during cruise AL595.

Date	AUV	Dive Name	Station	Start [UTC]	End [UTC]	Duration (hh:mm)
14.06.2023	Anton	Anton289	31	06:22h	09:20h	02:58
13.06.2023	Anton	Anton288	30	12:33h	17:10h	04:37
13.06.2023	Luise	Luise302	26	08:00h	11:47h	03:47
10.06.2023	Luise	Luise301	23	10:14h	09:30h	23:16
10.06.2023	Anton	Anton287	22	07:20h	12:05h	04:45
09.06.2023	Luise	Luise300	17	10:17h	14:24h	04:07
09.06.2023	Anton	Anton286	16	08:15h	12:39h	04:24
09.06.2023	Anton	Anton285	16	07:35h	07:57h	00:22
08.06.2023	Anton	Anton284	14	13:12h	17:34h	04:22
08.06.2023	Luise	Luise299	12	08:04h	09:18h	01:14
07.06.2023	Anton	Anton283	8	09:14h	12:01h	02:47
07.06.2023	Anton	Anton282	8	08:11h	08:53h	00:42
05.06.2023	Anton	Anton281	3	14:35h	15:21h	00:46
05.06.2023	Anton	Anton280	2	14:15h	14:18h	00:03

7 Data and Sample Storage and Availability

Data gathered during cruise AL595 are stored in facilities of GEOMAR Helmholtz Centre for Ocean Research Kiel and visible within the Ocean Science Information System (OSIS Kiel). All metadata are immediately available publicly via the following link pointing to OSIS Kiel (https://portal.geomar.de/kdmi#_48_INSTANCE_5P8d_=metadata%2Fleg%2Fshow%2F363087) in the GEOMAR data management portal. After a three year moratorium, the GEOMAR data management will assist to publish these data by dissemination to national and international data archives, i.e. the data will be submitted to PANGAEA or OSIS no later than October 2026. Sediment and rock samples will be stored at the Core and Rock Repository at GEOMAR in Kiel (responsible: Dr. Mark Schmidt). Genetic data will be made available over international servers (see table below).

Tab. 7.1 Overview of data availability.

Type	Database	Available	Free Access	Contact
Hydroacoustic data	PANGAEA / OSIS	10 / 2023	10 / 2026	gdy@geomar.de
CTD	PANGAEA / OSIS			
Genetic data	NCBI / EMBL			
Core samples (GC)	OSIS			

8 Acknowledgments

The Geomicrobiology and Biogeochemistry group is grateful for the help they received in preparing for the cruise (Hannes Schmidt) and providing sample processing equipment for the BIGO (Dr. Stefan Sommer), help with setting up the BIGO prior to the cruise (Asmus Petersen), and providing some of the vials and chemicals for the geochemical analyses (Betty Domeyer and Anke Bleyer). Further thanks go to the Icelandic Microbiologists for support in getting the permits. The scientific crew of cruise AL595 thank Captain Marc Petrikowski and his crew for their support throughout the entire cruise, which was a great help in conducting our experiments and contributed to the success of this cruise.

We thank the "Geschäftsstelle des Gutachterpanels Forschungsschiffe" and the anonymous reviewers for granting us the requested ship time and GEOMAR for providing funding of our cruise.

Cruise AL595 will contribute to the "Earth and Environment" Innovation Pool project "High CO_2 – metabolic responses and bioeconomic opportunities", in which FZ Jülich, GFZ Potsdam and GEOMAR are collaborating to study physiological adaptation of microbial communities and individual microbes to very high CO_2 concentrations and explore microbial utilization of CO_2 for establishing CO_2-based bioeconomic value chains.

9 References

Beaulieu, S.E., Baker, E.T., German, C.R., 2015: Where are the undiscovered hydrothermal vents on oceanic spreading ridges? Deep Sea Research Part II,121, 202–212.

Böhnke-Brandt, S., Sass, K., Gonnella, G., Diehl, A., Kleint, C., Zitoun, R. et al. (2019): Parameters governing the community structure and element turnover in Kermadec volcanic ash and hydrothermal fluids as monitored by inorganic electron donor consumption, autotrophic CO2 fixation and 16S tags of the transcriptome in incubation experiments. Front Microbio: DOI: 10.3389/fmicb.2019.02296.

Boschen, R.E., Rowden, A.A., Clark, M.R. & Gardner, J.P.A., 2013: Mining of deep-sea seafloor massive sulfides: A review of the deposits, their benthic communities, impacts from mining, regulatory frameworks and management strategies. Ocean and Coastal Management, 84, 54–67.

Botz, R., Winckler, G., Bayer, R., Schmitt, M., Schmidt, M., Garbe-Schönberg, D., Stoffers, P. & Kristjansson, J.K., 1999: Origin of trace gases in submarine hydrothermal vents of the Kolbeinsey Ridge, north Iceland. EPSL, 171, 83 – 93.

Dahle, H., Roalkvam, I., Thorseth, I.H., Pedersen, R.B., and Steen, I.H. (2013) The versatile in situ gene expression of an Epsilonproteobacteria-dominated biofilm from a hydrothermal chimney. Environ Microbiol Rep 5: 282-290.

Dahle, H., Okland, I., Thorseth, I.H., Pederesen, R.B., and Steen, I.H. (2015) Energy landscapes shape microbial communities in hydrothermal systems on the Arctic Mid-Ocean Ridge. Isme Journal 9: 1593-1606.

Devey, C. W. (2002): Cruise Report R.V. Poseidon Cruise Nr. 291 [POS291].

Eythorsdottir, A., Omarsdottir, S., and Einarsson, H. (2016) Antimicrobial Activity of Marine Bacterial Symbionts Retrieved from Shallow Water Hydrothermal Vents. Mar Biotechnol (NY) 18: 293-300.

Galley, A.G., Hannington, M. D. und Jonasson, I.R. (2007) Volcanogenic massive sulphide deposits Mineral Deposits of Canada: A Syntesis of Major Deposit Types. Geological Survey of Canada, Mineral Deposits Division Special Publication (5). Geological Association of Canada, St. John's, Newfoundland, pp. 141-162.

German, C.R., Petersen, S. & Hannington, M.D. (2016): Hydrothermal exploration of mid-ocean ridges: where might the largest sulfide deposits be forming? Chemical Geology, 420, 114-126.

Gonnella G., Böhnke S., Indenbirken D., Garbe-Schönberg D., Seifert R., Mertens C. et al (2016). Endemic hydrothermal vent species identified in the open ocean seed bank. Nature Microbiology 1: 16086.

Gudmundsdóttir, E.R., Eiríksson, J. & Larsen, G., 2011: Identification and definition of primary and reworked tephra in Late glacial and Holocene marine shelf sediments off North Iceland. J. Quat. Sci., 26, 589–602.

Gutierrez-Almada, K., Gonzalez-Acosta, B., Borges-Souza, J.M., and Aguila-Ramirez, R.N. (2020) Marine bacteria associated with shallow hydrothermal systems in the Gulf of California with the capacity to produce biofilm inhibiting compounds. Arch Microbiol 202: 1477-1488.

Han, Y.C., Gonnella, G., Adam, N., Schippers, A., Burkhardt, L., Kurtz, S. et al. (2018) Hydrothermal chimneys host habitat-specific microbial communities: analogues for studying the possible impact of mining seafloor massive sulfide deposits. Scientific Reports 8: 10386.

Hannington, M., Herzig, P., Stoffers, P., Scholten J., Botz, R. Garbe-Schönberg, D., Jonasson, I.R., Roest, W. & Shipboard Scientific Party, 2001: First observatons of high-termparature submarine hydrothermal vents and massive anhydrite deposits off the north coast of Iceland. Marine Geology, 177, 199 – 220.

Hannington, M.D., Jamieson, J., Monecke, T. & Petersen, S., 2010: Modern Sea-Floor Massive Sulfides and Base Metal Resources: Toward an Estimate of Global Sea-Floor Massive Sulfide Potential. Economic Geology Special Publication, 15, 317–338.

Hannington M., Jamieson, J., Monecke, T., Petersen, S. & Beaulieu, S., 2011: The abundance of seafloor massive sulfide deposits. Geology, 39, 1155-1158.

Hissmann, K., Rothenbeck, M., Wenzlaff, E., Weiß, T. und Leibold, P. (2020) RV ALKOR Fahrtbericht / Cruise Report AL533 - Mutual Field Trials of the Manned Submersible JAGO and the Hover-AUVs ANTON and LUISE off the Aeolian Islands, Mediterranean Sea, Catania (Italy) – La Seyne-sur-mer (France) 05.02. – 18.02.2020. Open Access. GEOMAR Report, N. Ser. 055. GEOMAR Helmholtz-Zentrum für Ozeanforschung Kiel, Kiel, Germany, 43 pp. DOI 10.3289/GEOMAR_REP_NS_55_2020.

Hölz, S. & Martins, S. (eds): RV POSEIDON Fahrtbericht / Cruise Report POS524 - GrimseyEM: Geophysical and geological investigations in the vicinity of the Grimsey Hydrothermal Field offshore Northern Iceland for the assessment of the geothermal potential and the exploration for potential mineralizations within the seafloor, Reykjavik (Iceland) – Bergen (Norway), 7.6 - 26.6.2018. Open Access. GEOMAR Report, N. Ser. 044. GEOMAR Helmholtz-Zentrum für Ozeanforschung, Kiel, Germany, 69 pp, 2018. DOI 10.3289/CR_POS524.

Hölz, S., Haroon, A. & Martins, S., eds. (2019): RV POSEIDON Fahrtbericht / Cruise Report POS535 - Loki2GrimseyEM: Geophysical and geological investigations of massive sulfides at and in the vicinity of Loki's Castle (Norway) and similar experiments around the Grimsey Hydrothermal Field (Iceland) for the assessment of the geothermal potential and the exploration for potential mineralizations within the seafloor. Akureyri (Iceland) – Bremerhaven (Germany), 09.06 – 03.07.2019. GEOMAR Report, N. Ser. 0053. GEOMAR Helmholtz-Zentrum für Ozeanforschung, Kiel, Germany, 89pp. DOI 10.3289/GEOMAR_REP_NS_53_2019.

Huber, J.A., Cantin, H.V., Huse, S.M., Welch, D.B.M., Sogin, M.L., and Butterfield, D.A. (2010) Isolated communities of Epsilonproteobacteria in hydrothermal vent fluids of the Mariana Arc seamounts. FEMS Microbiol Ecol, 73, 538-549.

Imachi, H., Nobu, M.K., Nakahara, N., Morono, Y., Ogawara, M., Takaki, Y. et al. (2020) Isolation of an archaeon at the prokaryote-eukaryote interface. Nature, 577, 519-525.

IMO (2018a): Icelandic Met Office - 400 earthquakes detected at Grímsey island in last 12 hours. Electronic pub., icelandmonitor.mbl.is/news/nature_and_travel/2018/02/15/400_earthquakes_detected_at_grimsey_island_in_last_, accessed 26.3.18.

IMO (2018b): Icelandic Met Office - Seismic swarm near Grímsey: update 15:00, 19 February. WWW electronic publication, accessed 26.3.2018, http://en.vedur.is/about-imo/news/seismic-swarm-near-grimsey-update-15-00-19-february.

Kicklighter, C.E., Fisher, C.R., and Hay, M.E. (2004) Chemical defense of hydrothermal vent and hydrocarbon seep organisms: a preliminary assessment using shallow-water consumers. Mar Ecol Prog Ser, 275, 11-19.

Lackschewitz, K.S., Botz, R., Garbe-Schönberg, D., Scholten, J. & Stoffers, P., 2006: Mineralogy and geochemistry of clay samples from active hydrothermal vents off the north coast of Iceland. Marine Geology, 225, 177 – 190.

Magnúsdóttir, S., Brandsdóttir, B. Driscoll, N. & Detrick, R., 2015: Postglacial tectonic activity within the Skjálfandadjúp Basin, Tjörnes Fracture Zone, offshore Northern Iceland, based on high resolution seismic stratigraphy. Marine Geology, 367, 159 – 170.

Monecke, T., Petersen, S., Hannington, M.D., Grant, H. & Samson, I., 2016: The Minor Element Endowment of Modern Sea-Floor Massive Sulfides and Comparison with Deposits Hosted in Ancient Volcanic Successions. In: Rare Earth and Critical Elements in Ore Deposits, Society of Economic Geologists, 2016.

Olins, H.C., Rogers, D.R., Preston, C., Ussler, W., Pargett, D., Jensen, S. et al. (2017) Co-registered Geochemistry and Metatranscriptomics Reveal Unexpected Distributions of Microbial Activity within a Hydrothermal Vent Field. Front Microbio 8: 1042.

Pedersen, R.B., Thorseth, I.H., Bygård, T.E. (2010a): Hydrothermal activity along the Arctic mid-ocean ridge. In: Diversity of Hydrothermal, Systems on Slow-Spreading Ocean Ridges, Geophys. Monogr. 188, edited by P. Rona et al., AGU, Washington, D. C., 2010.

Pedersen, R.B., Rapp, H.T., Thorseth, I.H., Lilley, M.D., Barriga, F.J., Baumberger, T., Flesland, K., Fonseca, R., Früh-Green, G.L. & Jorgensen, S.L. (2010b): Discovery of a black smoker vent field and vent fauna at the Arctic Mid-Ocean Ridge. Nature Communications, 1 (126), 1-6.

Perner, M., Gonnella, G., Hourdez, S., Böhnke, S., Kurtz, S., and Girguis, P. (2013a) In-situ chemistry and microbial community compositions in five deep-sea hydrothermal fluid samples from Irina II in the Logatchev field. Environ Microbiol 15: 1551-1560.

Perner, M., Hansen, M., Seifert, R., Strauss, H., Koschinsky, A., and Petersen, S. (2013b) Linking geology, fluid chemistry and microbial activity of basalt- and ultramafic-hosted deep-sea hydrothermal vent environments Geobiology 11: 340-355.

Riedel, C., Schmidt, M., Botz, R. & Theilen F., 2001: The Grimsey hydrothermal field offshore North Iceland: Crustal structure, faulting and related gas venting. Earth and Planetary Science Letters, 193 (3-4), 409-421.

Scholten, J., Shipboard Scientific Party, 2000: Cruise Report of R/V Poseidon 253, Institute for Geosciences, Departments of Geophysics and Geology-Paleontology, Universtity of Kiel, 42pp.

Shi, Y., Pan, C., Auckloo, B.N., Chen, X., Chen, C.A., Wang, K. et al. (2017) Stress-driven discovery of a cryptic antibiotic produced by Streptomyces sp. WU20 from Kueishantao hydrothermal vent with an integrated metabolomics strategy. Appl Microbiol Biotechnol 101: 1395-1408.

Snow, J.E. & Edmonds, H.N., 2007: Ultraslow-spreading ridges rapid paradigm changes. Oceanography, 20, 90-101.

Sommer, S., Gier, J., Treude, T., et al (2016) Depletion of oxygen, nitrate and nitrite in the Peruvian oxygen minimum zone cause an imbalance of benthic nitrogen fluxes. Deep Sea Research Part I: Oceanographic Research Papers 112:113±122. doi: 10.1016/j.dsr.2016.03.001.

Sommer, S., Linke, P., Pfannkuche, O., Schleicher, T., Schneider v. Deimling, J., Reitz, A., Haeckel, M., Flögel, S., Hensen, C. (2009) Seabed methane emissions and the habitat of frenulate tubeworms on the Captain Arutyunov mud volcano (Gulf of Cadiz). Mar Ecol Prog Ser 382, 69- 86.

Spang, A., Saw, J.H., Jorgensen, S.L., Zaremba-Niedzwiedzka, K., Martijn, J., Lind, A.E. et al. (2015) Complex archaea that bridge the gap between prokaryotes and eukaryotes. Nature 521: 173-+.

Steen, I.H., Dahle, H., Stokke, R., Roalkvam, I., Daae, F.L., Rapp, H.T. et al. (2016) Novel Barite Chimneys at the Loki's Castle Vent Field Shed Light on Key Factors Shaping Microbial Communities and Functions in Hydrothermal Systems. Front Microbio 6.

Stokke, R., Dahle, H., Roalkvam, I., Wissuwa, J., Daae, F.L., Tooming-Klunderud, A. et al. (2015) Functional interactions among filamentous Epsilonproteobacteria and Bacteroidetes in a deep-sea hydrothermal vent biofilm. Environ Microbiol 17: 4063-4077.

10 Abbreviations

AMOR	Arctic Mid-Ocean Ridge
AUV	Autonomous Underwater Vehicle
BIGO	Biogeochemical Observatory
CTD	Conductivity temperature depth
DIC	Dissolved inorganic carbon
DOC	Dissolved organic carbon
DTM	dissolved trace metal analyses
DVL	Doppler Velocity Log
EM	Electromagnetic
FisH	Fluorescence in situ Hybridization
GC	Gravity Coring / Gravity Corer
GVF / GHF	Grimsey Vent Field / Grimsey Hydrothermal Field
IC	Ion chromatography
ICP-OES	Inductively coupled plasma optical emission spectrometry
LBL	Long baseline
MNP	Marine Natural Product (research)
MOR	Mid-Ocean Ridge
MUC	Multi corer
MS	Mass spectroscopy / mass spectrometer
PEC	Polyestercarbonat
PI	Principal Investigator
PP	Polypropylen
PW	porewater
SMS	Seafloor massive sulfides
TA	Total alkalinity

11 Appendices

11.1 Core Descriptions

Full core descriptions are pending work. They will be created at GEOMAR after the cruise.

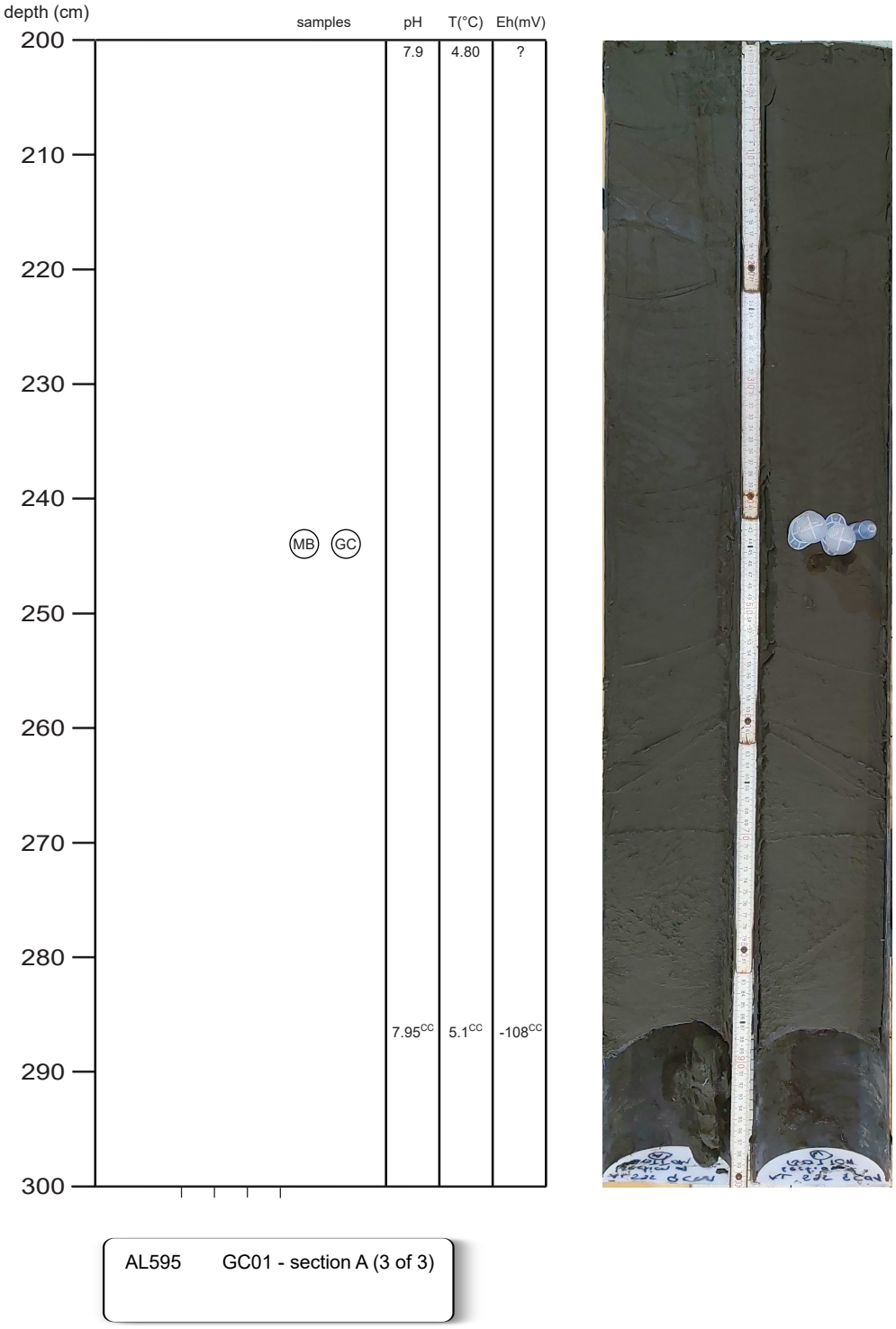

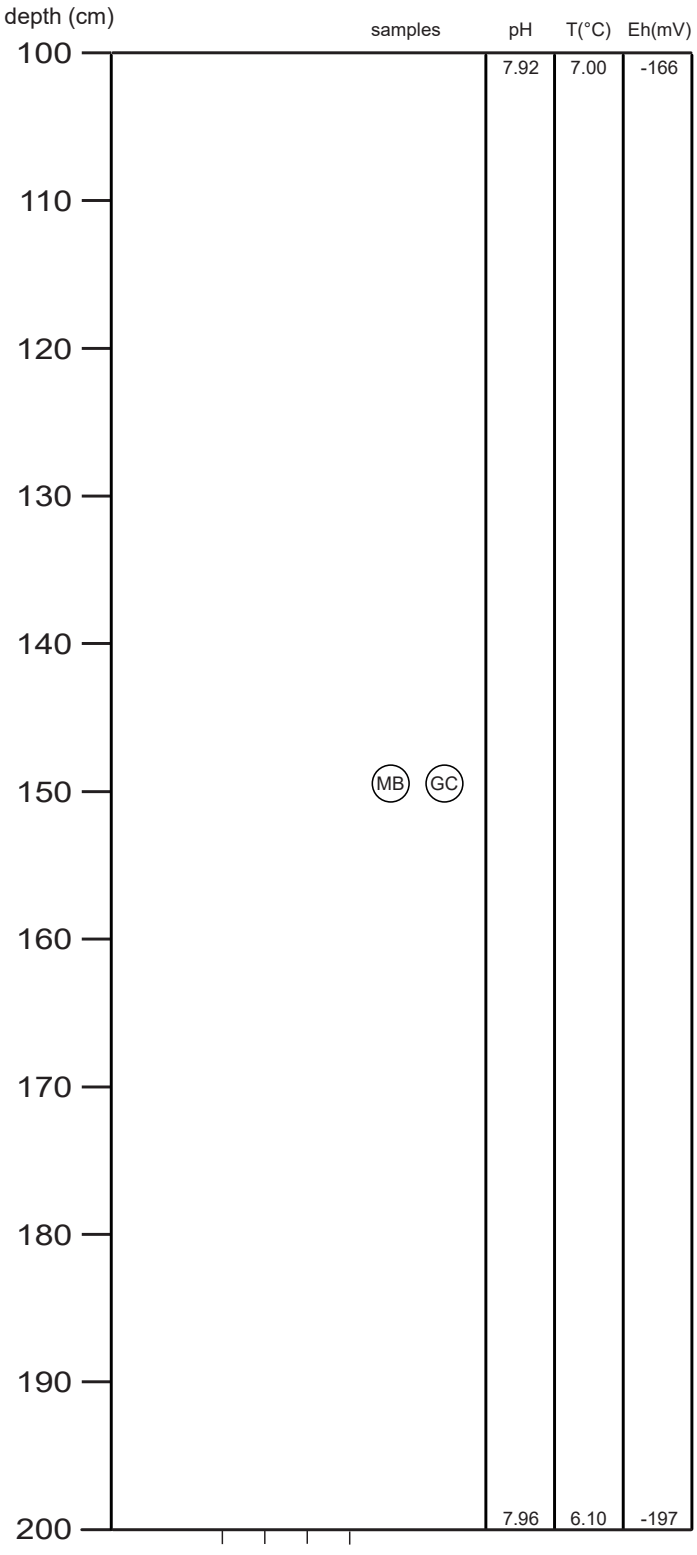

AL595 GC01 - section B (2 of 3)

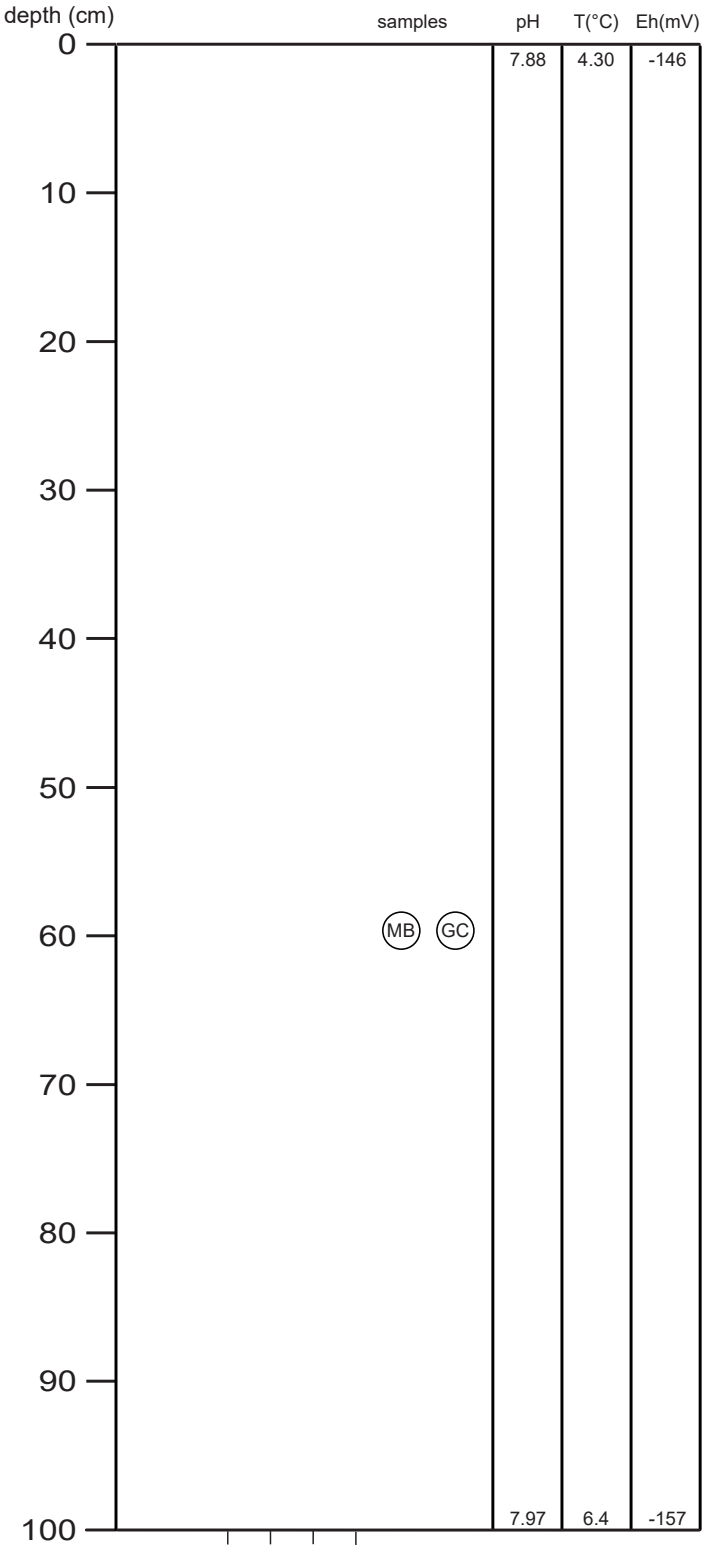

AL595 GC01 - section C (1 of 3)

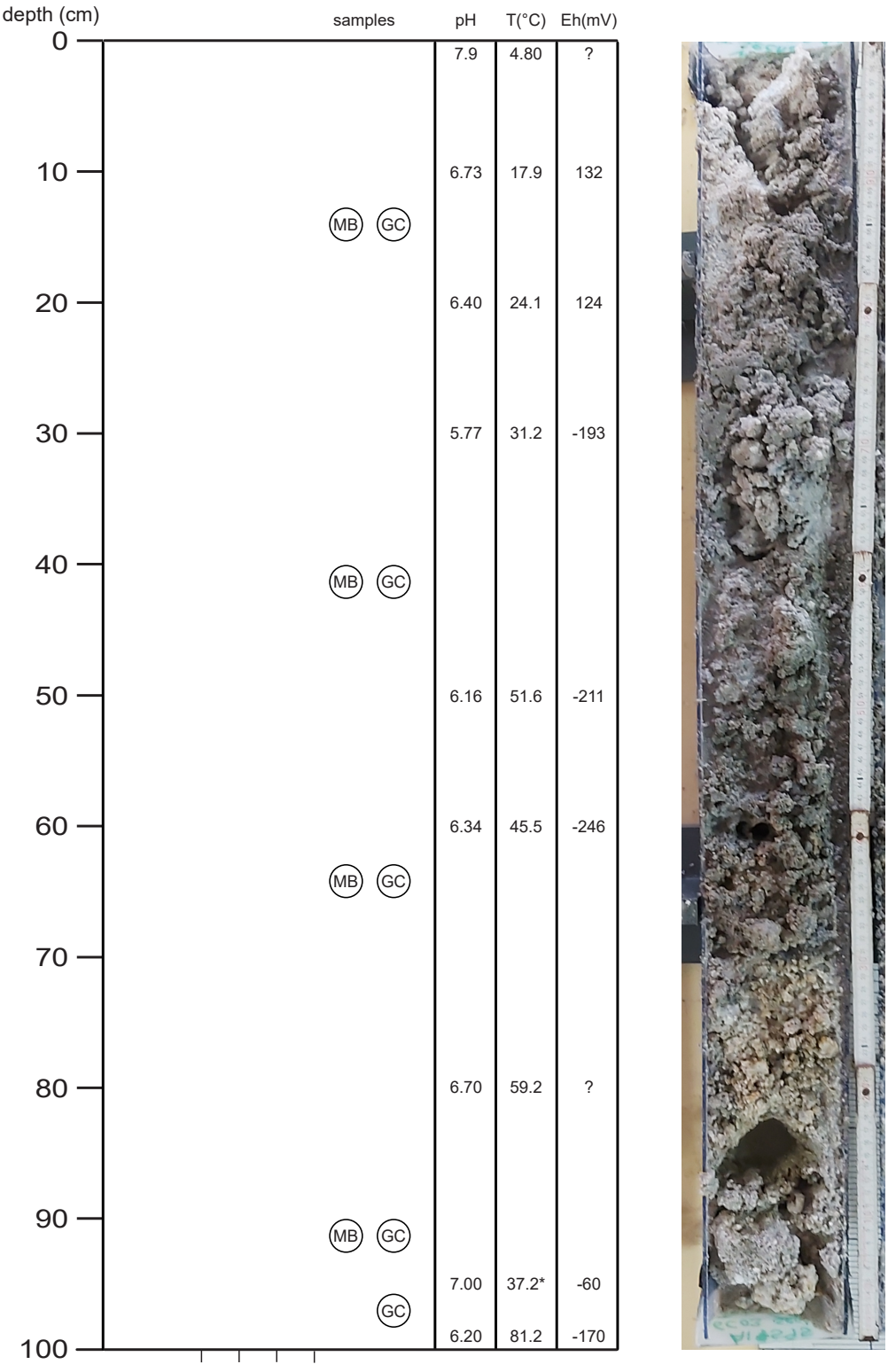

AL595 GC03 - section A (1 of 1)

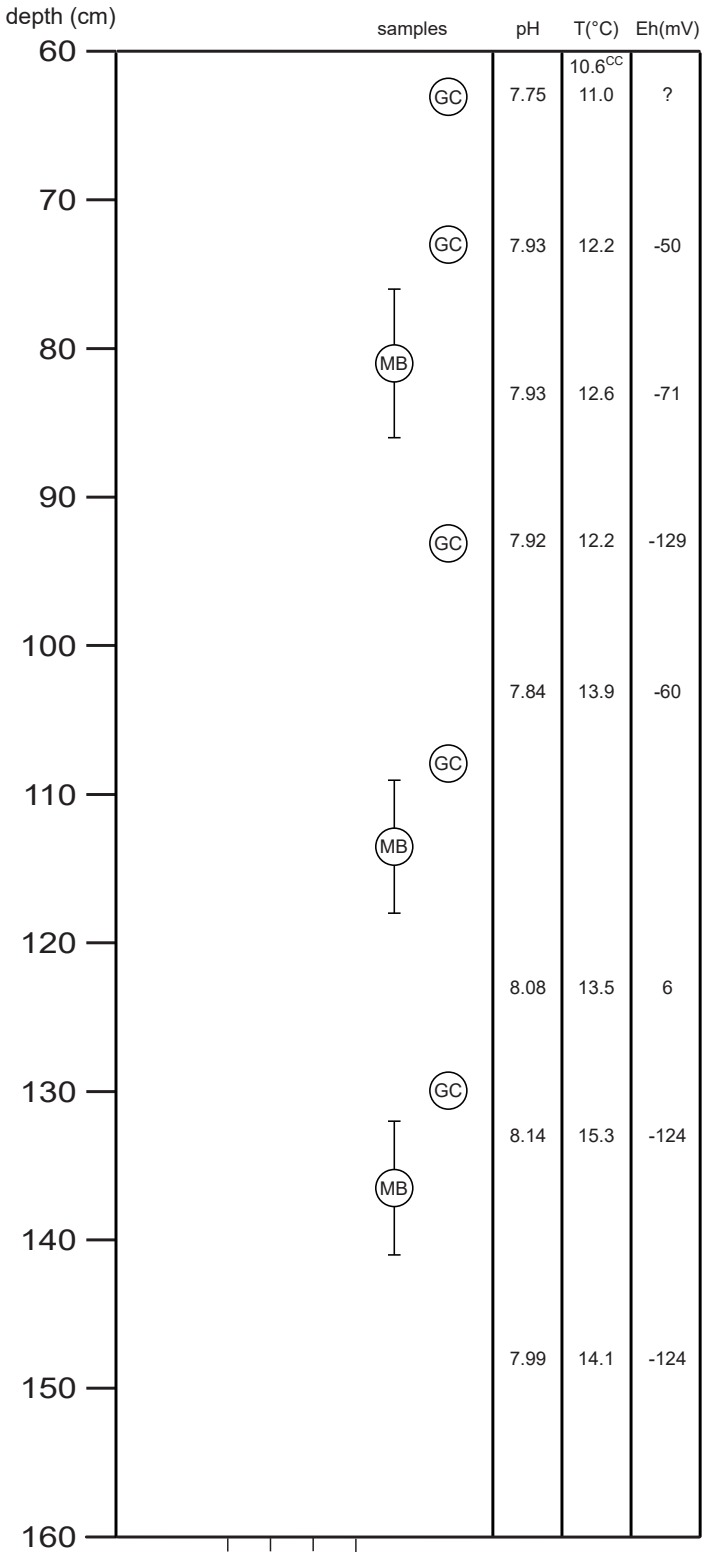

AL595 GC04 - section A (2 of 2)

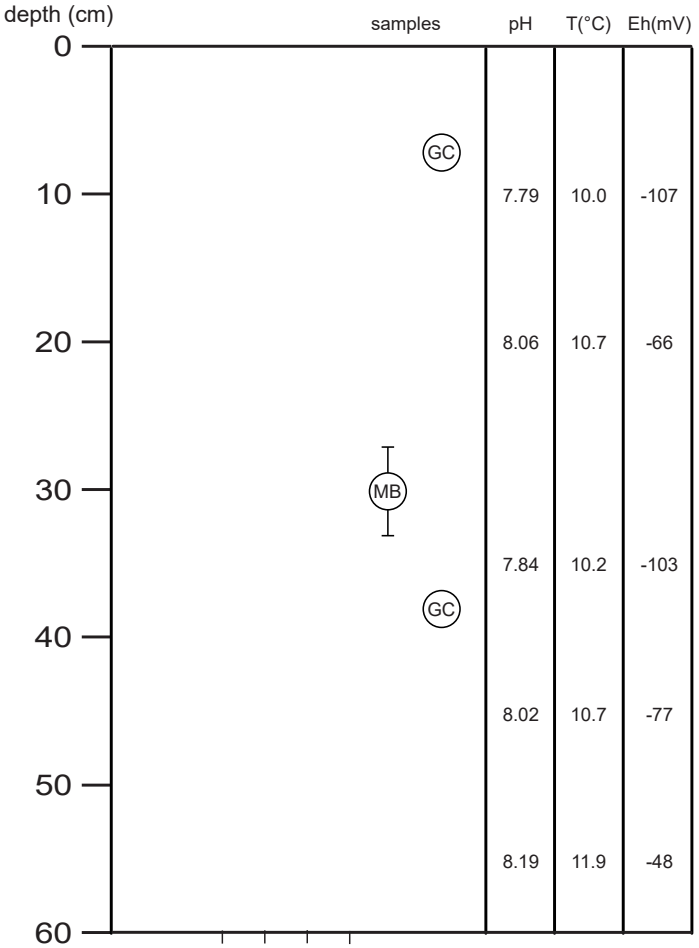

AL595 GC04 - section B (1 of 2)

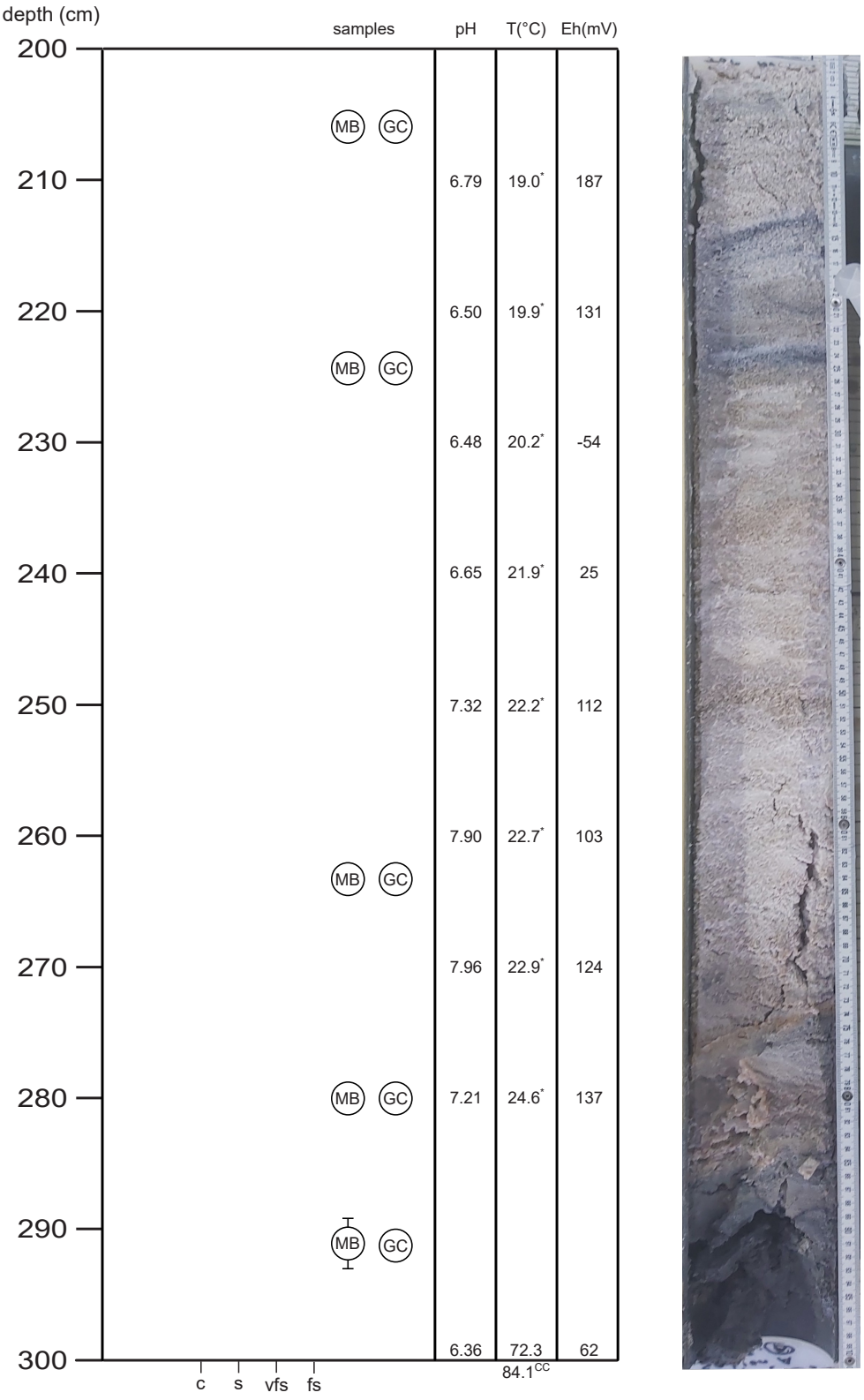

AL595 GC05 - section A (3 of 3)

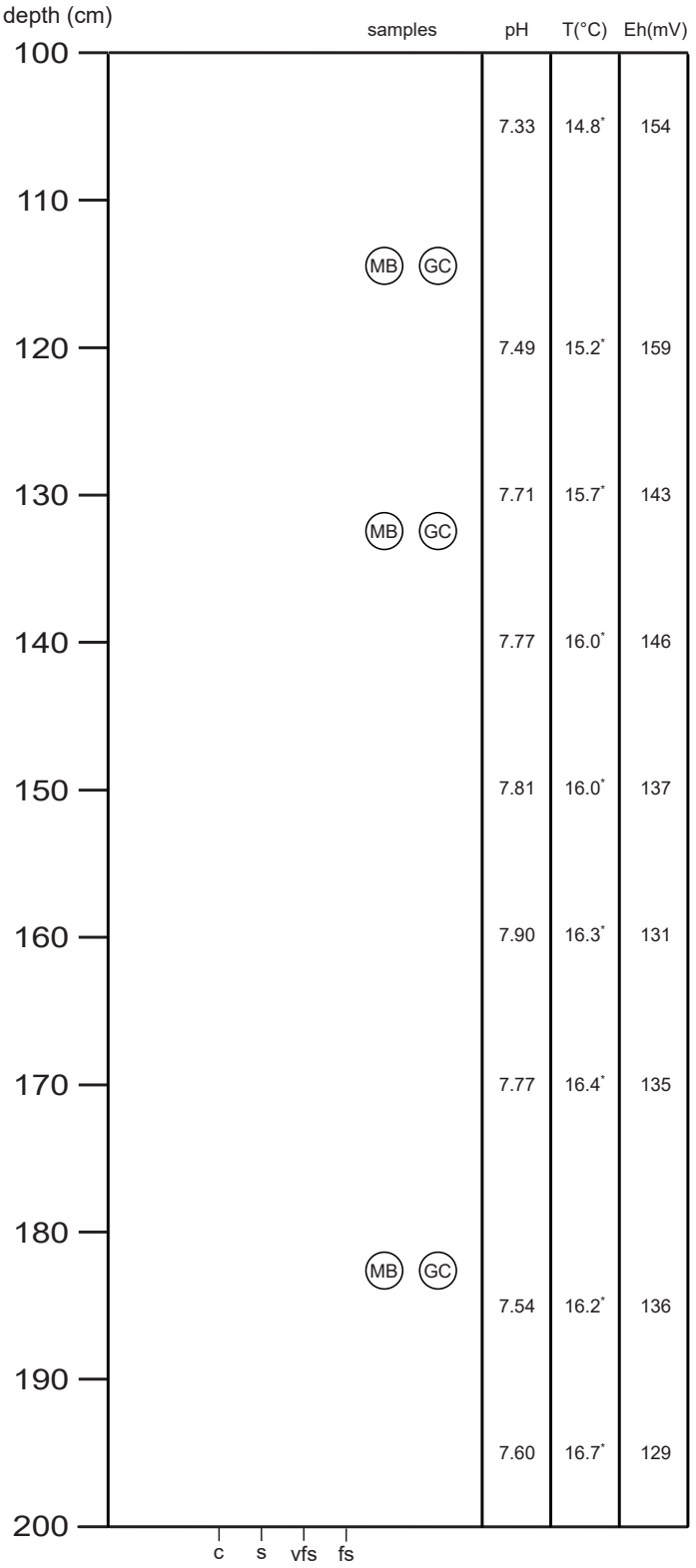

AL595 GC05 - section B (2 of 3)

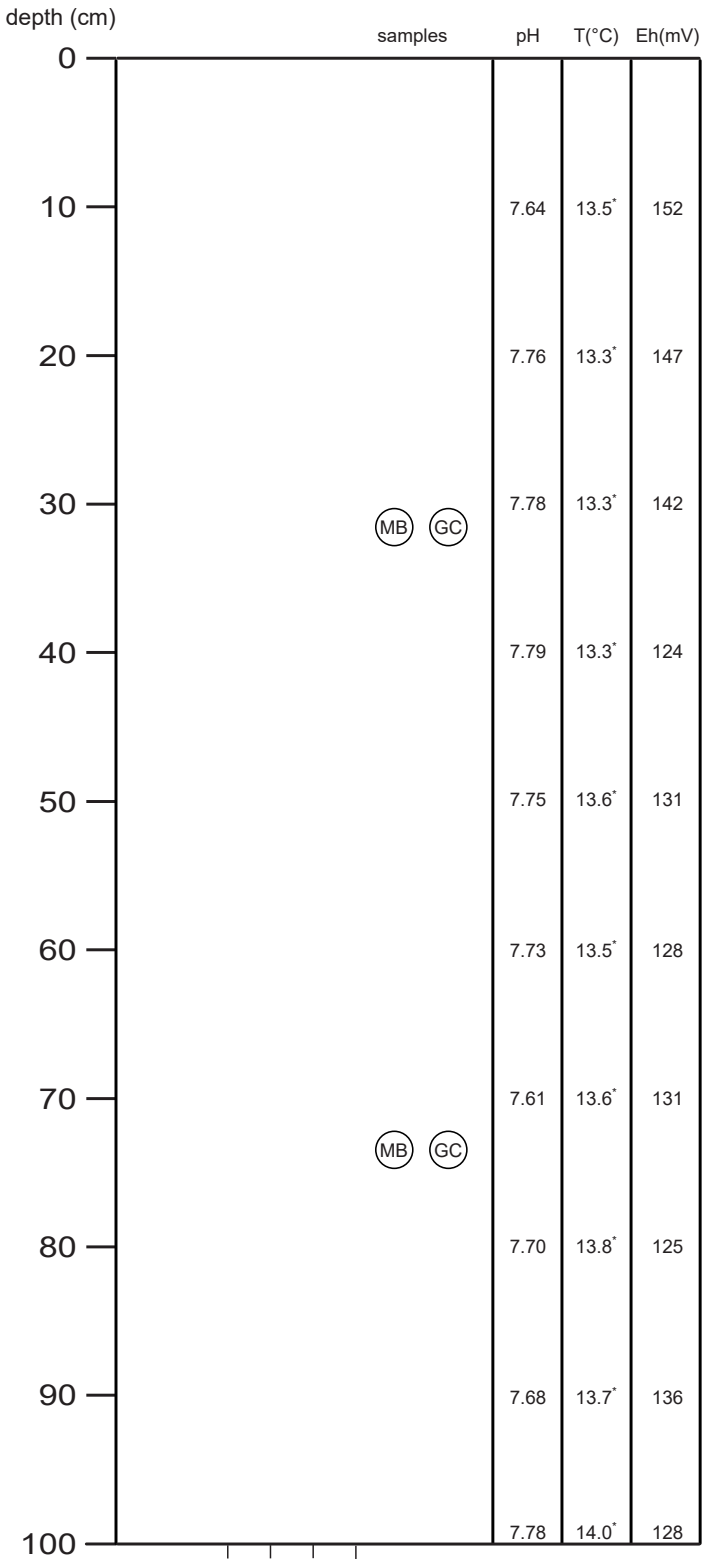

AL595 GC05 - section C (1 of 3)

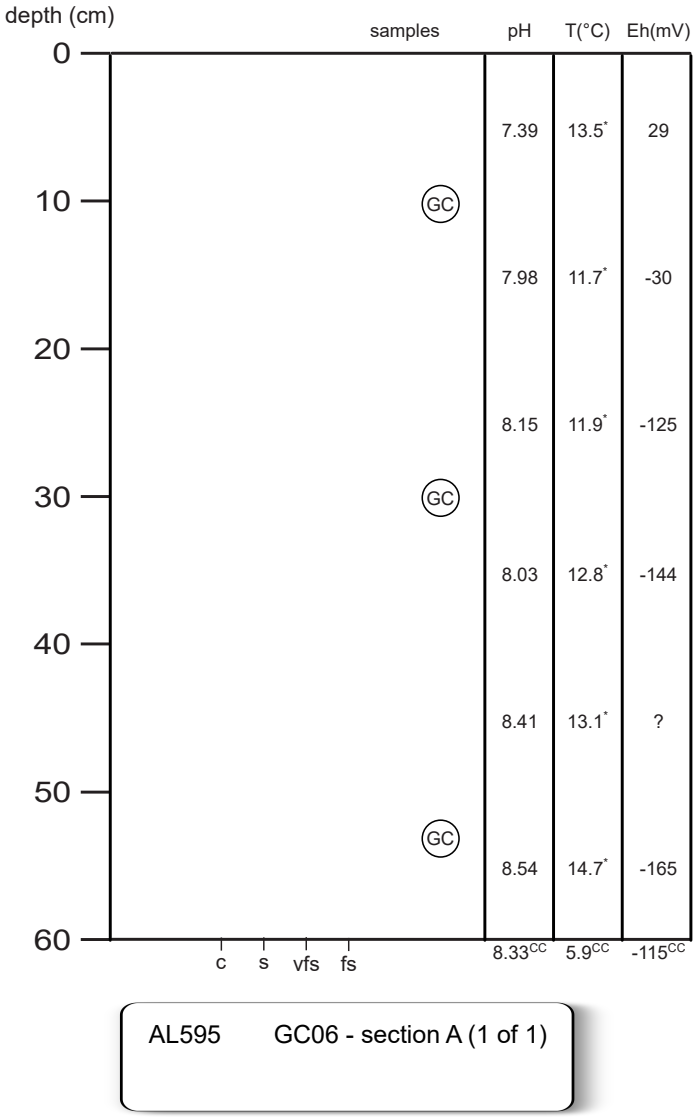

AL595 GC06 - section A (1 of 1)

11.2 List of Samples

11.2.1 Geomicrobiology and Biogeochemistry

MUC01 reference, no temperature measured (cold), same location as GC01, 6.6.2023													
Liner	**Sample**	**Depth [cm]**	**PW vol. [ml]**	**TA**	**IC**	**H_2S (ZnAc 5%)**	**Fe (6M HCl)**	**DIC / DOC ($HgCl_2$)**	**FisH (FA 4%)**	**RNA/DNA -80°C**	**Fe Extraction (from solid phase)**	**Headspace (# of bottle)**	**porosity**
1	1	0-1	Not measured	2x	x	x	x	x	x	x	x	No headspace	x
	2	1-2		x	x	x	x	x	x	x	x		x
	3	2-3		x	x	x	x	x	x	x	x		x
	4	3-4		x	x	x	x	x	x	x	x		x
	5	4-6		x	x	x	x	x	x	x	x		x
	6	6-8		2x	x	x	x	x	x	x	x		x
	7	8-10		x	x	x	x	x	x	x	x		x
	8	10-12		x	x	x	x	x	x	x	x		x
	9	12-14		2x	x	x	x	x	x	x	x		x
	10	14-16		x	x	x	x	x	x	x	x		x
	11	16-18		x	x	x	x	x	x	x	x		x
	12	18-20		x	x	x	x	x	x	x	x		x
	13	20-22		2x	x	x	x	x	x	x	x		x
	14	22-24		x	x	x	x	No DIC	x	x	x		x
	15	24-26		x	x	x	x	x	x	x	x		x
	16	26-28		x	x	x	x	x	x	x	x		x
	17	28-30		x	x	x	x	x	x	x	x		x
	18	30-32		x	x	x	x	x	x	x	x		x
	19	32-35		x	x	x	x	x	x	x	x		x
	20	35-38		2x	x	x	x	x	x	x	x		x

MUC03 was not sampled for geomicrobiology and biogeochemistry.

MUC04 vent field, 16°C, same location as GC05, 13.06.2023													
Liner	**Sample**	**Depth [cm]**	**PW vol. [ml]**	**TA**	**IC**	**H_2S (ZnAc 5%)**	**Fe (6M HCl)**	**DIC / DOC ($HgCl_2$)**	**FisH (FA 4%)**	**RNA/DNA -80°C**	**Fe Extraction (from solid phase)**	**Headspace (# of bottle)**	**porosity**
1	1	0-2	11	x	x	2x	x	x	x	x	x	1	x
	2	2-4	6	x	x	x	x	x	x	x	x	2	x
	3	4-6	9	x	x	x	x	x	x	x	x	3	x
	4	6-8	11	x	x	x	x	x	x	x	x	4	x
	5	8-10	13	x	x	x	x	x	x	x	x	5	x
	6	10-12	9	x	x	x	x	x	x	x	x	6	x
	7	12-14	8	x	x	x	x	x	x	x	x	7	x
	8	14-17	12	x	x	x	x	x	x	x	x	8	x
	9	17-20	12	x	x	x	x	x	x	x	x	9	x
	10	20-23	12	x	x	x	x	x	x	x	x	10	x
	11	23-26	11	x	x	x	x	x	x	x	x	11	x
	12	26-30	9	x	x	x	x	x	x	x	x	12	x

GC01 reference, total length 300cm, same location as MUC01, 7.6.2023													
Section	**Sample**	**Depth [cm]**	**PW vol. [ml]**	**TA**	**IC**	**H_2S (ZnAc 5%)**	**Fe (6M HCl)**	**DIC / DOC ($HgCl_2$)**	**FisH (FA 4%)**	**RNA/DNA -80°C**	**Fe Extraction (from solid phase)**	**Headspace (# of bottle)**	**porosity**
A	GC1-1	244	4	x	x	x	x	No DIC	x	x	x	No headspace	x
B	GC1-2	150	7,5	x	x	x	x		x	x	x		x
C	GC1-3	60	5	x	x	x	x		x	x	x		x

GC03 vent field, total length 99cm, T_{max} = 71.6°C, core also sampled by matís for MNP (same sample numbers), 08.06.2023													
Section	**Sample**	**Depth [cm]**	**PW vol. [ml]**	**TA**	**IC**	**H_2S (ZnAc 5%)**	**Fe (6M HCl)**	**DIC / DOC ($HgCl_2$)**	**FisH (FA 4%)**	**RNA/DNA -80°C**	**Fe Extraction (from solid phase)**	**Headspace (# of bottle)**	**porosity**
A	GC3-1	12-16	17	x	x	x	x	x	x	x	x	#1	x
	GC3-2	40-42	14	x	x	x	x	x	x	x	x	#2	x
	GC3-3	63-67	14,5	x	x	x	x	x	x	x	x	#3	x
	GC3-4	90-92	9	x	x	x	x	x	x	x	x	#4	x

GC04 vent field, total length 150cm, T_{max} = 15.3°C, core also sampled by matís for MNP (same sample numbers), 09.06.2023													
Section	**Sample**	**Depth [cm]**	**PW vol. [ml]**	**TA**	**IC**	**H_2S (ZnAc 5%)**	**Fe (6M HCl)**	**DIC / DOC ($HgCl_2$)**	**FisH (FA 4%)**	**RNA/DNA -80°C**	**Fe Extraction (from solid phase)**	**Headspace (# of bottle)**	**porosity**
B	GC4-1	27-33	16	x	x	x	x	x	x	x	x	#5	x
A	GC4-2	76-86	6	x	x	x	x		x	x	x	#6	x
	GC4-3	109-118	6	x	x	x	x		x	x	x	#7	x
	GC4-4	132-141	6	x	x	x	x		x	x	x	#8	x

GC05 vent field, total length 300cm, T_{max} = 84.1°C, same location as MUC04, 13.06.2023													
Section	**Sample**	**Depth [cm]**	**PW vol. [ml]**	**TA**	**IC**	**H_2S (ZnAc 5%)**	**Fe (6M HCl)**	**DIC / DOC ($HgCl_2$)**	**FisH (FA 4%)**	**RNA/DNA -80°C**	**Fe Extract. (from solid phase)**	**Headspace (# of bottle)**	**porosity**
C	GC5-10	30-32	Nd	x	x	x	x	x	x	x	x	13	x
	GC5-9	72-75	Nd	x	x	x	x	x	x	x	x	14	x
	GC5-8	113-116	19	x	x	x	x	x	x	x	x	15	x
	GC5-7	131-134	15	x	x	x	x	x	x	x	x	16	x
	GC5-6	181-184	13	x	x	x	x	x	x	x	x	17	x
B	GC5-5	205-207	10	x	x	x	x	x	x	x	x	18	x
	GC5-4	223-225	10	x	x	x	x	x	x	x	x	19	x
	GC5-3	262-265	16	x	x	x	x	x	x	x	x	20	x
A	GC5-2	279-282	10	x	x	x	x	x	x	x	x	21	x
	GC5-1	289-293	6	x	x	x	x	x	x	x	x	22	x

GC06 was not sampled for geomicrobiology and biogeochemistry.

11.2.2 Marine Natural Product Research

Sample	CTD	bottle	Depth [cm]	Amount [ml]	Sample processing		
					plating	-80°C storage filtration (0.45µm)	4°C storage (backup), 15ml
W1-1	CTD01	1	399	2500	x	x	x
W1-2	CTD01	10	399	2500	x	x	x
W2-1	CTD02	1	374	2500	x	x	x
W2-2	CTD02	10	374	2500	x	x	x
W3-1	CTD03	1	375	2500	x	x	x
W3-2	CTD03	2	375	2500		x	x
W4-1	CTD04	1	370	2500	x	x	x
W4-2	CTD04	2	370	2500		x	x
W7-1	CTD07	2	374	2500	x	x	x
W7-2	CTD07	3	374	2500		x	x

Sample	Core	Liner	Depth [cm]	Sample processing			
				plating	4°C storage (backup), 1.5ml	-80°C storage for DNA	-80°C storage 20% Glycerol
S1-1	MUC01	2	soft layer above sediment	x	x	x	x
S1-2			0-1cm	x	x	x	x
S1-3			3-4cm	x	x	x	x
S1-4			6-7cm	x	x	x	x
S1-5			9-10cm	x	x	x	x
S1-6			19-20cm	x	x	x	x
S1-7			39-40cm	x	x	x	x
O1		1	Polychaeta from top	x	x	x	
S3-1	MUC02[2]	1	soft layer above sediment	x	x		
S3-2			0-1cm	x	x	x	x
S3-3			3-4cm	x	x	x	x
S3-4			6-7cm	x	x	x	x
S3-5			9-10cm	x	x	x	x
S3-6			19-20cm	x	x	x	x
S3-7			39-40cm	x	x	x	x
S7-1	MUC04	2	soft layer above sediment	x	x	x	
S7-2			0-1cm	x	x	x	x
S7-3			3-4cm	x	x	x	x
S7-4			6-7cm	x	x	x	x
S7-5			9-10cm	x	x	x	x
S7-6			19-20cm	x	x	x	x
S7-7			29-30cm	x	x	x	x

2 Five samples (Sample 1 – 5) were taken at depths of 0cm, 10cm, …, 40cm for analyses at matís (Iceland).

11.2.3 Geochemistry

Sample	Core / section	Depth [cm]	Porewater [ml]	DTM+ICP [ml]	Hg Fluid [ml]	Nutrients [ml]	Hg Sediment	Solid Matter	Extra ICP [ml]
AL595_PW_01	GC01/C	60	x	3	2	2	x	x	
AL595_PW_02	GC01/B	150	x	3	2	2	x	x	
AL595_PW_03	GC01/A	244	x	3	2	2	x	x	
AL595_PW_04	GC03/A	12-16	21	3	2	3	x	x	3
AL595_PW_05	GC03/A	40-42	21	3	2	3	x	x	3
AL595_PW_06	GC03/A	63-67	21	3	2	3	x	x	3
AL595_PW_07	GC03/A	90-92	21	3	2	3	x	x	3
AL595_PW_08	GC03/A	97	21	3	2	3	x	x	3
AL595_PW_09	GC04/B	7	21	3	2	3	x	x	
AL595_PW_10	GC04/B	38	21	3	2	3	x	x	3
AL595_PW_11	GC04/A	63	19	3	2	3	x	x	
AL595_PW_12	GC04/A	73	20	3	2	3	x	x	2
AL595_PW_13	GC04/A	93	15	3	2	3	x	x	
AL595_PW_14	GC04/A	108	7	3	1	2	x	x	1
AL595_PW_15	GC04/A	130	20	3	2	3	x	x	1
AL595_PW_16	GC05/C	30-32	20	3	2	2	x	x	
AL595_PW_17	GC05/C	72-75	20	3	2	2	x	x	
AL595_PW_18	GC05/B	113-116	20	3	2	2	x	x	
AL595_PW_19	GC05/B	131-134	20	3	2	2	x	x	
AL595_PW_20	GC05/B	181-184	20	3	2	2	x	x	
AL595_PW_21	GC05/A	205-207	20	3	2	2	x	x	
AL595_PW_22	GC05/A	223-225	20	3	2	2	x	x	
AL595_PW_23	GC05/A	262-265	20	3	2	2	x	x	
AL595_PW_24	GC05/A	279-282	20	3	2	2	x	x	
AL595_PW_25	GC05/A	289-293	12	3	2	2	x	x	
AL595_PW_26	GC06/A	10	21	3	2	2	x	x	
AL595_PW_27	GC06/A	30	21	3	2	2	x	x	
AL595_PW_28	GC06/A	53	10	3	2	2	x	x	

Sample	Core / Liner	Depth [cm]	Porewater [ml]	DTM+ICP [ml]	Hg Fluid [ml]	Nutrients [ml]	Hg Sediment	Solid Matter	Comments
AL595_PW_29	MUC01.1	0-1	x	3	1	1			
AL595_PW_30	MUC01.1	1-2	x	3					
AL595_PW_31	MUC01.1	2-3	x	3					
AL595_PW_32	MUC01.1	3-4	x	3					
AL595_PW_33	MUC01.1	4-6	x	3					
AL595_PW_34	MUC01.1	6-8	x	3	1	1			taken with metal spatula
AL595_PW_35	MUC01.1	8-10	x	3					
AL595_PW_36	MUC01.1	10-12	x	3					
AL595_PW_37	MUC01.1	12-14	x	3	1	1			
AL595_PW_38	MUC01.1	14-16	x	3					
AL595_PW_39	MUC01.1	16-18	x	3					
AL595_PW_40	MUC01.1	18-20	x	3					
AL595_PW_41	MUC01.1	20-22	x	3	1	1			
AL595_PW_42	MUC01.1	22-24	x	3					
AL595_PW_43	MUC01.1	24-26	x	3					
AL595_PW_44	MUC01.1	26-28	x	3					
AL595_PW_45	MUC01.1	28-30	x	3					
AL595_PW_46	MUC01.1	30-32	x	3					
AL595_PW_47	MUC01.1	32-35	x	3					
AL595_PW_48	MUC01.1	35-38	x	3	1	1			
AL595_PW_49	MUC01.2	1					x	x	
AL595_PW_50	MUC01.2	10					x	x	
AL595_PW_51	MUC01.2	20					x	x	
AL595_PW_52	MUC01.2	30					x	x	
AL595_PW_53	MUC01.2	40					x	x	
AL595_PW_54	MUC04.1	bottom water	x	3					
AL595_PW_55	MUC04.1	0-2	x	3					
AL595_PW_56	MUC04.1	2-4	x	3					
AL595_PW_57	MUC04.1	4-6	x	3					
AL595_PW_58	MUC04.1	6-8	x	3					

Sample	Core / Liner	Depth [cm]	Porewater [ml]	DTM+ICP [ml]	Hg Fluid [ml]	Nutrients [ml]	Hg Sediment	Solid Matter	Comments
AL595_PW_59	MUC04.1	8-10	x	3					
AL595_PW_60	MUC04.1	10-12	x	3					
AL595_PW_61	MUC04.1	12-14	x	3					
AL595_PW_62	MUC04.1	14-17	x	3					
AL595_PW_63	MUC04.1	17-20	x	3					
AL595_PW_64	MUC04.1	20-23	x	3					
AL595_PW_65	MUC04.1	23-26	x	3					
AL595_PW_66	MUC04.1	26-30	x	3					
AL595_PW_67	MUC04.2	0-2	14	3	2	2	x	x	
AL595_PW_68	MUC04.2	7-9	14	3	2	2	x	x	
AL595_PW_69	MUC04.2	14-16	15	3	2	2	x	x	
AL595_PW_70	MUC04.2	21-23	16	3	2	2	x	x	
AL595_PW_71	MUC04.2	28-30	11	3	2	2	x	x	

BIGO01					BIGO02				
Sample	**Core / Chamber**	**Depth [cm]**	**Porewater [ml]**	**DTM+ICP [ml]**	**Sample**	**Core / Chamber**	**Depth [cm]**	**Porewater [ml]**	**DTM+ICP [ml]**
AL595_PW_72	BIGO1/1	bottom water	x	3	AL595_PW_91	BIGO2	Niskin	x	3
AL595_PW_73	BIGO1/1	0-1	x	3	AL595_PW_92	BIGO2/1	bottom water	x	3
AL595_PW_74	BIGO1/1	1-2	x	3	AL595_PW_93	BIGO2/1	0-2	x	3
AL595_PW_75	BIGO1/1	2-3	x	3	AL595_PW_94	BIGO2/1	2-4	x	3
AL595_PW_76	BIGO1/1	3-4	x	3	AL595_PW_95	BIGO2/1	4-6	x	3
AL595_PW_77	BIGO1/1	4-6	x	3	AL595_PW_96	BIGO2/1	6-8	x	3
AL595_PW_78	BIGO1/1	6-8	x	3	AL595_PW_97	BIGO2/1	8-10	x	3
AL595_PW_79	BIGO1/1	8-10	x	3	AL595_PW_98	BIGO2/1	10-12	x	3
AL595_PW_80	BIGO1/1	10-12	x	3	AL595_PW_99	BIGO2/1	12-14	x	3
AL595_PW_81	BIGO1/1	12-14	x	3	AL595_PW_100	BIGO2/1	14-16	x	3
AL595_PW_82	BIGO1/1	14-15	x	3	AL595_PW_101	BIGO2/2	bottom water	x	3
AL595_PW_83	BIGO1/2	bottom water	x	3	AL595_PW_102	BIGO2/2	0-2	x	3
AL595_PW_84	BIGO1/2	0-1	x	3	AL595_PW_103	BIGO2/2	2-4	x	3
AL595_PW_85	BIGO1/2	1-2	x	3	AL595_PW_104	BIGO2/2	4-6	x	3
AL595_PW_86	BIGO1/2	2-3	x	3	AL595_PW_105	BIGO2/2	6-8	x	3
AL595_PW_87	BIGO1/2	3-4	x	3	AL595_PW_106	BIGO2/2	8-10	x	3
AL595_PW_88	BIGO1/2	4-6	x	3	AL595_PW_107	BIGO2/2	10-12	x	3
AL595_PW_89	BIGO1/2	6-8	x	3	AL595_PW_108	BIGO2/2	12-14	x	3
AL595_PW_90	BIGO1/2	8-10	x	2					

11.3 AUV – Photogrammetry

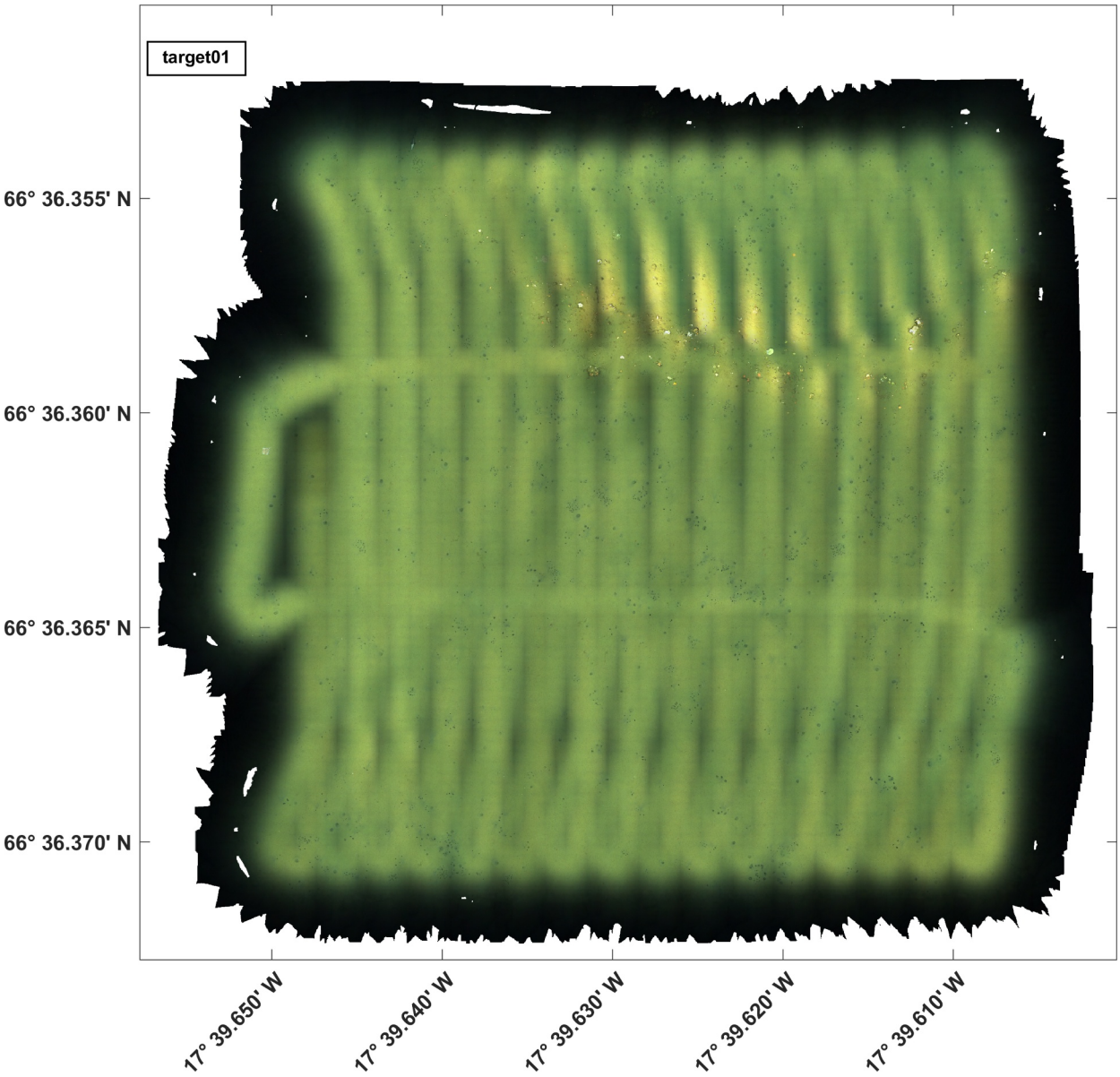

Fig. 11.1 Photo-mosaic of target01, for location see map in Fig. 5.19 (p. 35). Vertical stripe patterns (and two horizontal stripes) are acquisition artifacts and need to be handled in post-processing.

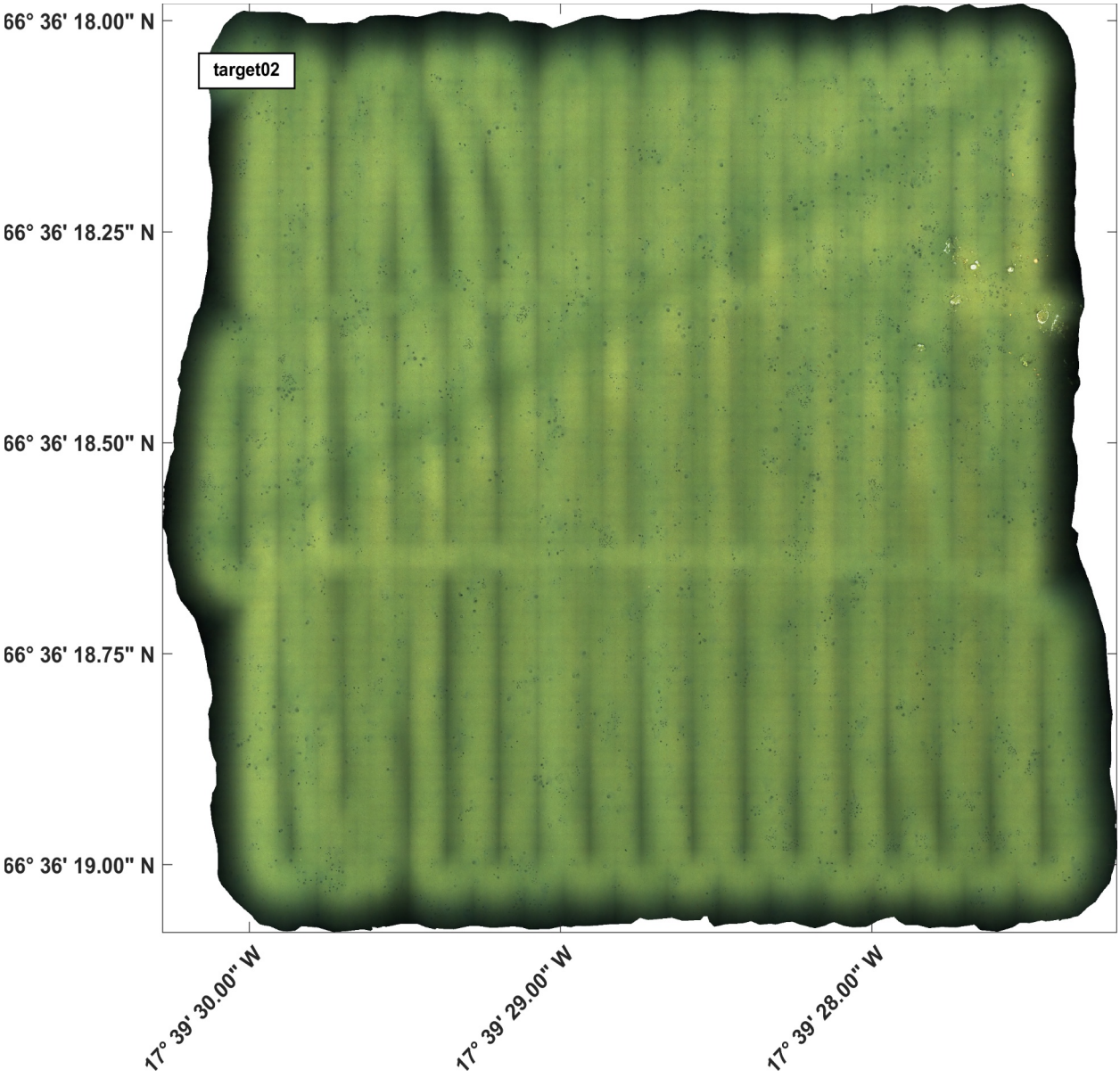

Fig. 11.2 Photo-mosaic of target02, for location see map in Fig. 5.19 (p. 35). Vertical stripe patterns (and two horizontal stripes) are acquisition artifacts and need to be handled in post-processing. WSW ↔ ENE striking stripes are most likely due to trawl nets.

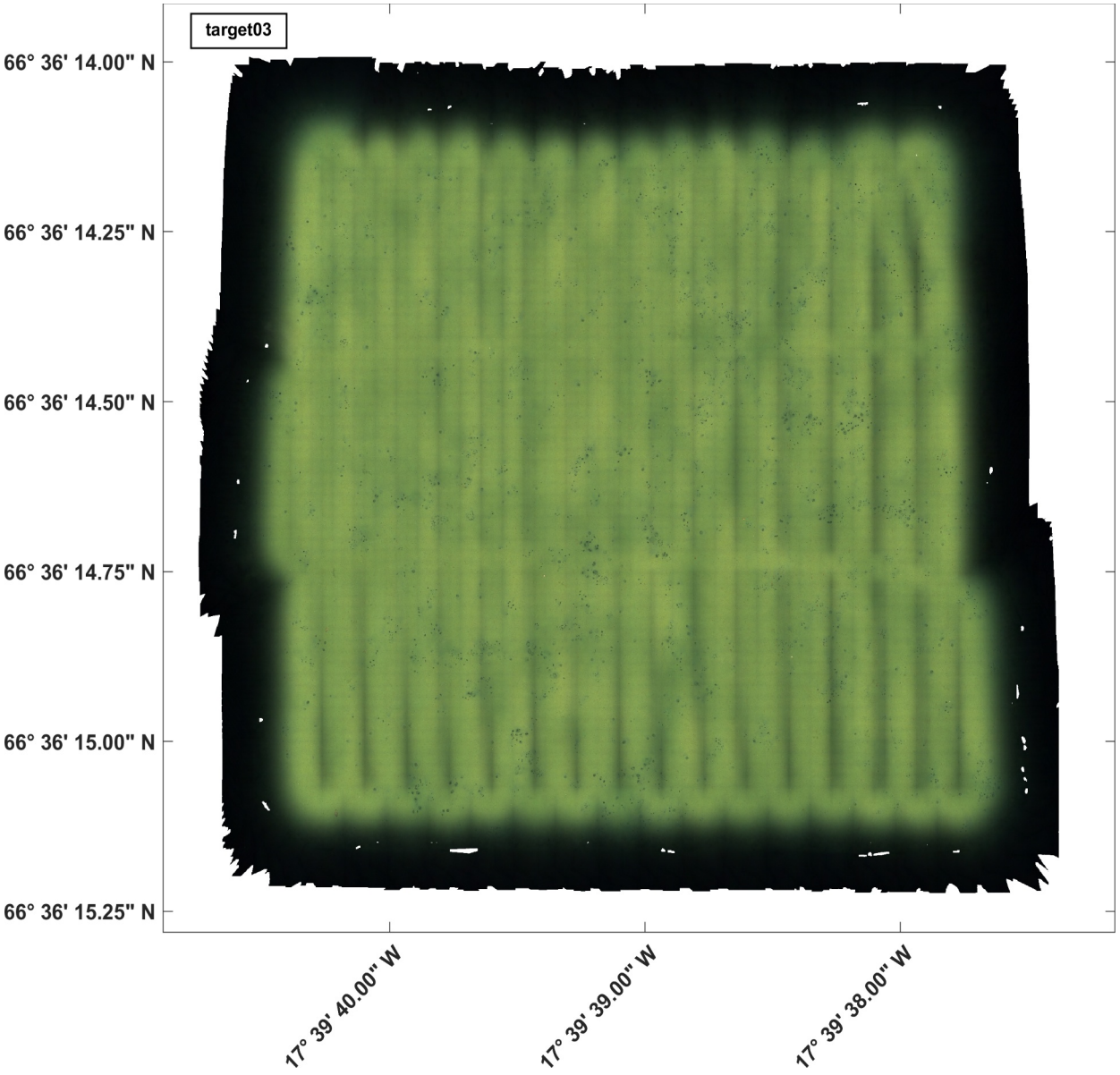

Fig. 11.3 Photo-mosaic of target03, for location see map in Fig. 5.19 (p. 35). Vertical stripe patterns are acquisition artifacts and need to be handled in post-processing.

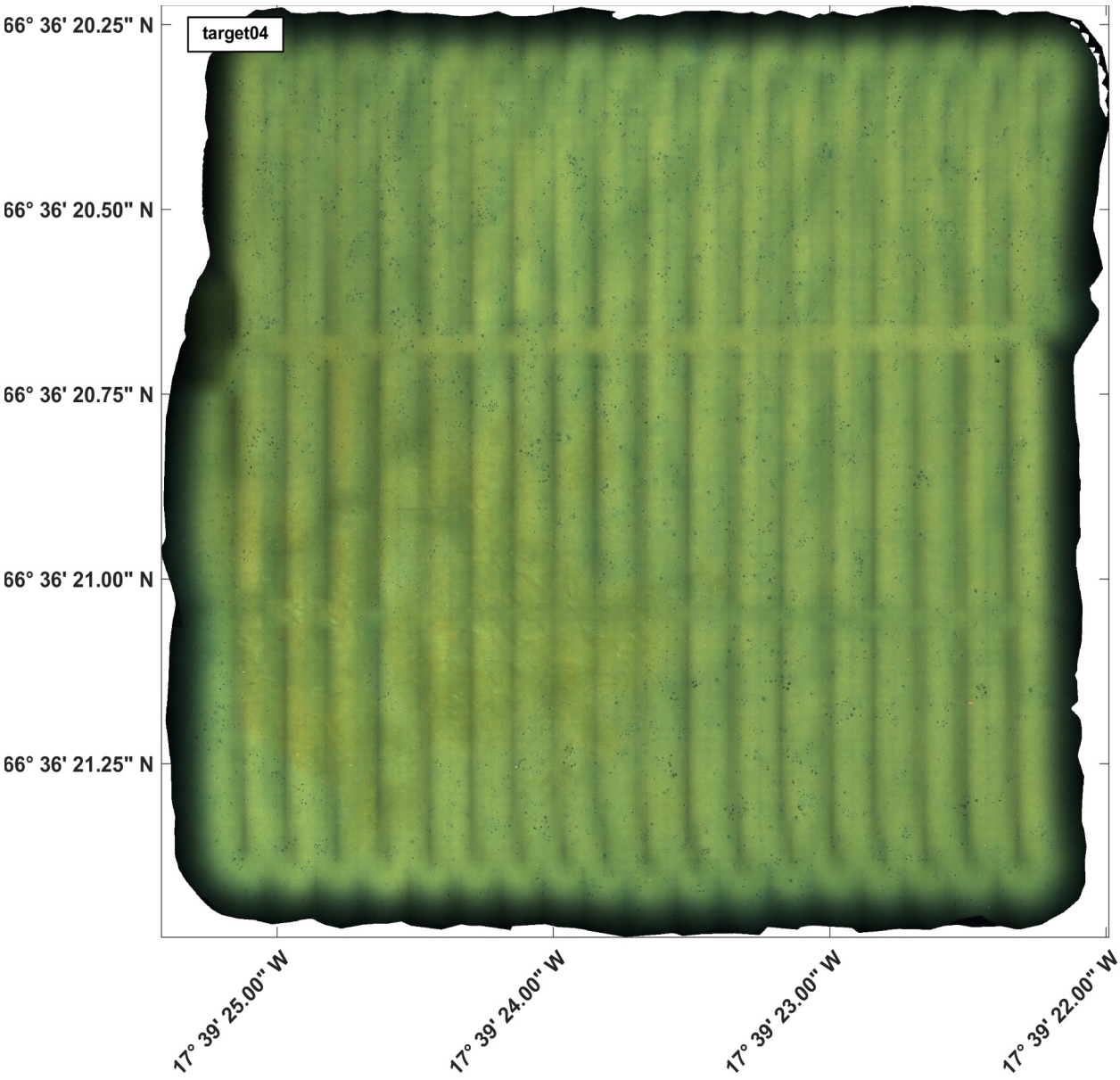

Fig. 11.4 Photo-mosaic of target04 (BIGO), for location see map in Fig. 5.19 (p. 35). Vertical stripe patterns (and two horizontal stripes) are acquisition artifacts and need to be handled in post-processing. Stripes at different angles are most likely due to fishing nets.

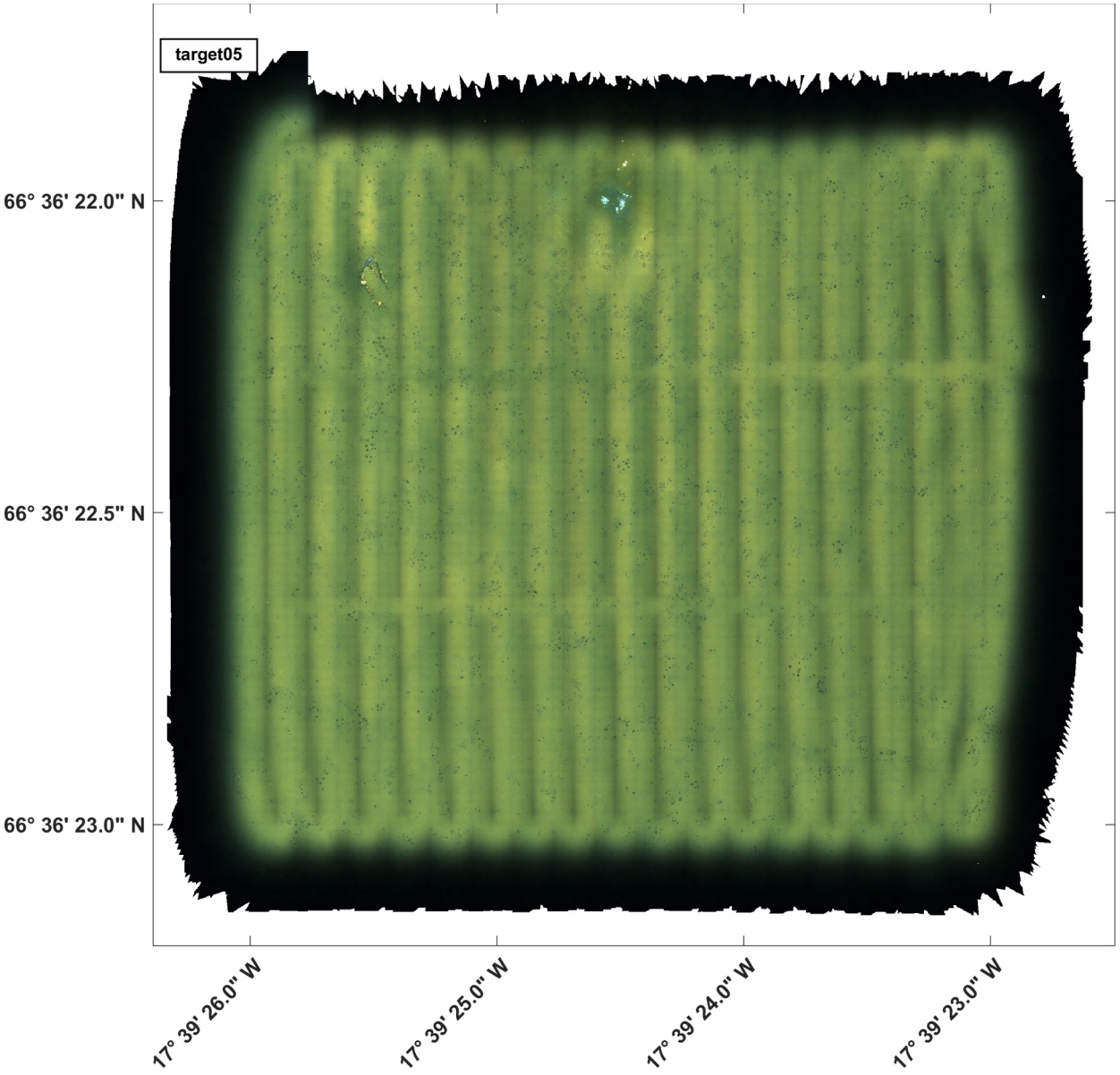

Fig. 11.5 Photo-mosaic of target05, for location see map in Fig. 5.19 (p. 35). Vertical stripe patterns (and two horizontal stripes) are acquisition artifacts and need to be handled in post-processing.